12-2019

Understanding how the Effectors HopD1 and HopG1 from the Bacterial Pathogen Pseudomonas syringae pv. tomato DC3000 target the Arabidopsis thaliana Protein AtNHR2B to cause Disease in Plants

Catalina Maria Rodriguez Puerto
University of Arkansas, Fayetteville

Understanding how the Effectors HopD1 and HopG1 from the Bacterial Pathogen *Pseudomonas syringae* pv. tomato DC3000 target the *Arabidopsis thaliana* Protein AtNHR2B to cause Disease in Plants

A thesis submitted in partial fulfillment
of the requirements for the degree of
Master of Science in Plant Pathology

by

Catalina Maria Rodríguez Puerto
Pontificia Universidad Javeriana
Bachelor of Science in Biology, 2017

December 2019
University of Arkansas

This thesis is approved for recommendation to the Graduate Council.

_____
Clemencia M. Rojas, Ph.D.
Thesis Director

_____
Jeffrey Lewis, Ph.D.
Committee Member

_____
Martin Egan, Ph.D.
Committee Member

Abstract

The pathogenicity of *Pseudomonas syringae* is associated with the type III secretion system (T3SS), a complex of proteins assembled in the inner and outer bacterial membranes that traverses the plant cell wall to deliver bacterial proteins into the cytoplasm of plant cells. The effector proteins translocated into the plant cells are called Hops (Hypersensitive response and pathogenicity outer proteins). Bacterial effectors target plant immune proteins to suppress defense responses and enhance bacterial parasitism. The *Arabidopsis thaliana* nonhost resistance 2B (AtNHR2B), a recently identified immune protein, is degraded after inoculation with the adapted pathogen of *Arabidopsis*, *P. syringae* pv tomato DC3000 (*Pst* DC3000), but not by the non-adapted pathogen *P. syringae* pv. tabaci (*Pstab*). Several *Pst* DC3000 effectors, including HopG1 and HopD1 interact with AtNHR2B *in planta*. Characterization of the effectors presence in plants upon inoculation with *Pstab* showed that transgenic expression of *HopG1-FLAG* triggered cell death, high electrolyte leakage levels and increased production of mitochondrial ROS. In contrast, *HopG1-FLAG* expression in combination with *AtNHR2B-GFP* caused susceptibility to *Pstab* as shown by the development of disease symptoms and the significant increase in bacterial growth. Together, these results suggest that HopG1 targets AtNHR2B to interfere with plant immune response upon bacterial infection. In contrast, transgenic plants expressing *HopD1-HA* alone or in combination with *AtNHR2B-GFP*, showed disease symptoms after inoculation with *Pstab*, that normally does not cause disease in wild-type Col-0 plants. Moreover, *Pstab* grew significantly more in transgenic plants overexpressing *HopD1-HA* than in wild-type Col-0. Interestingly, *Arabidopsis* plants expressing the bacterial effector *HopD1-HA* alone or in combination with *AtNHR2B-GFP* were deficient in callose deposition and showed a downregulation of the callose synthase gene *PMR4*. Altogether, these results suggest that HopD1 interferes with callose deposition and by doing so hinders defense responses.

Acknowledgements

I would like to thank my advisor Dr. Clemencia Rojas for her guidance and support throughout my masters, as well as Dr. Raksha Singh for training me in the laboratory and for giving me her friendship.

I would also like to thank my committee members Dr. Martin Egan and Dr. Jeffrey Lewis and all the people in the Department of Plant Pathology and Entomology at the University of Arkansas.

Dedication

I would like to dedicate this thesis to my parents who have thought me that hard work always pays off, who have loved me and care for me unconditionally. To my sisters, for their love and all the laughs.

Table of Contents

1 Introduction

1.1 *Pseudomonas syringae*: an Ubiquitous Plant Pathogenic Bacterium

Gram-negative plant pathogenic bacteria belonging to the genera *Pseudomonas*, *Ralstonia*, *Agrobacterium*, *Xanthomonas* and *Erwinia,* have been recognized as significant plant pathogens as they cause diseases in economically important crops (Mansfield et al., 2012; Buttner, 2016). Within the genus *Pseudomonas,* the species *Pseudomonas syringae* is considered a major plant pathogen due to its ability to cause disease in a large number of crop plants including tomato, wheat, rice, bean, soybean, kiwi, hazelnut and tobacco, among many others (**http://www.pseudomonas-syringae.org/**). Because of this broad host range, the *P. syringae* species has been further divided into pathovars based on their host specificity, and up to 50 different pathovars have been described (Xin et al., 2018). Examples of some diseases caused by specific pathovars are: "Wildfire on tobacco" caused by *P. syringae* pv. tabaci; "Halo blight on beans" caused by *P. syringae* pv. phaseolicola “Bacterial blight of soybeans” caused by *P. syringae* pv. glycinea, and "Bacterial Speck of tomato" caused by *P. syringae* pv. tomato DC3000 (*Pst* DC3000) (Lindeberg et al., 2012). *Pst* DC3000 also infects the model plant *Arabidopsis thaliana* and, this pathosystem has become a model to understand bacterial pathogenicity in plants.

1.2 Disease Cycle of *P. syringae*

P. syringae infections of plants occurs in two phases: the first phase is the epiphytic phase, wherein bacterial survives and multiplies on the surface of the plant tissue. This phase occurs in the aerial plant organs such as flowers, fruits, leaves and stems. The second phase is the endophytic phase that occurs when bacteria enter the plant and colonizes the intercellular space known as the apoplast (Xin et al., 2018). Significant bacterial multiplication in the apoplast with

concurrent expression of pathogenicity genes leads to the development of disease and the appearance of visible symptoms (Xin et al., 2018).

P. syringae disease cycle is dependent on humidity, which is necessary for *P. syringae* to survive and multiply during the epiphytic phase. In the field, humidity associated with dew, fog or rain during the growing season, has been responsible for disease outbreaks (Xin et al., 2018).

1.3 Virulence Factors in *P. syringae*

Several virulence factors have been identified and characterized in *P. syringae* and include phytotoxins, extracellular polysaccharides, the plant hormone auxin and a myriad of proteins secreted by the type III secretion system.

Phytotoxins

As a species, *P. syringae* produces at least 13 different toxins with several modes of action. Among them, coronatine, syringomycin, syringopeptin, tabtoxin, and phaseolotoxin have been well characterized (Bender et al., 1999). The most studied phytotoxin is coronatine and, it is produced by *P. syringae* pv. tomato DC3000 as well as by *P. syringae* pv. glycinea. The presence of this toxin is required for the complete virulence of these pathovars in their respective host plants. Coronatine results from the combination of coronafacic acid and coronamic acid and its production is associated with the chlorotic symptoms observed in the diseases caused by the pathovars that produced it. Purified coronatine causes chlorosis in every plant when exogenously applied, and for that reason it is considered a nonhost-specific toxin (Bender et al., 1999). At early stages of pathogenesis, coronatine contributes to the virulence of *P. syringae* by inhibiting stomatal closure upon bacterial recognition, and consequently promotes bacterial entry into the plant tissue (Melotto et al., 2008).

Syringomycin contributes to the development of disease symptoms due to is ability to disrupt plant cell membranes and cause leakage of cell contents, which promotes a wet plant surface that increases bacterial mobility (Bender et al., 1999).

Extracellular polysaccharides (EPS)

Exopolysaccharides (EPS) are polymers formed by sugar residues that protect bacteria from harsh environmental conditions (Laue et al., 2006). EPS provides protection, enhances the attachment of bacteria to surfaces and can be used as a nutrient source (Keith et al., 2003) .

P. syringae secretes two EPS: levan and alginate. Levan is synthesized by the bacteria when sucrose is available, and that is presumed to be a reservoir of carbohydrates and source of nutrients during starvation periods (Laue et al., 2006), but their role in pathogenicity is not known. Alginate is produced in association with the disease cycle, when there are conditions of high humidity on the leaf surface. Alginate is required for *P. syringae* to survive the epiphytic phase of its life cycle (Keith et al., 2003). Alginate also confers protection against desiccation and toxic molecules, and its production has been associated with the development of water-soaked lesions on infected leaves (Fett and Dunn, 1989; Laue et al., 2006).

Auxin

Auxin is a plant hormone involved in plant growth and developmental processes, such as cell division and elongation and fruit and flower formation (Duca et al., 2014). The indole-3-acetic acid (IAA), is also produced by plant-associated bacteria (Glickmann et al., 1998; Aragon et al., 2014) and contributes to bacterial pathogenesis. For example, *P. syringae* pv savastonoi also known as *Pseudomonas savastonoi* pv. savastonoi produces tumors in woody plants associated with the production of IAA (Gardan et al., 1992).

Pseudomonas syringae pv. syringae B728a, causal agent of the bacterial brown spot disease in bean also uses the IAA as a virulence factor. *P. syringae* pv. syringae B728a harbors the gene Psyr_0007 that encodes the enzyme arylacetonitrilase that uses compounds like indole-3-acetonitrile (IAN) and phenylpropionitrile (PPN) as nitrogen sources to synthesize IAA (Howden et al., 2009). Psyr_0007 is also present in the *Pst*DC3000 genome, however it is not functional in this *P. syringae* pathovars (Howden et al., 2009). *Pst*DC3000 produces IAA through a different biosynthetic pathway that two aldehyde dehydrogenases (ALD): AldA and AldB, that use tryptophan as precursor (McClerklin et al., 2018). In *Pst*DC3000 IAA is a known virulence factor that enhances susceptibility of *A. thaliana* plants presumably by interfering with the function of defense plant hormones like salicylic acid (SA) (Mutka et al., 2013; McClerklin et al., 2018).

Type III secretion system

Although *P. syringae* produces several virulence factors, the most important of them is the type III secretion system (T3SS), a complex of proteins that delivers bacterial proteins inside eukaryotes. The T3SS is one of several secretion systems encoded by Gram-negative bacteria that is essential for pathogenicity towards plants or animals (Costa et al., 2015), and therefore, is conserved in diverse genera of animal pathogens such as *Escherichia*, *Salmonella*, *Shigella and Yersinia* as well as in diverse genera of plant pathogens such as *Erwinia, Pseudomonas*, *Ralstonia* and *Xanthomonas* (Buttner, 2016).

In animal and plant pathogens, the T3SS apparatus is a macromolecular structure that resembles a syringe and is made by 25 different proteins. The base of the apparatus is made by a stack of rings spanning the bacterial inner and outer membranes. This base extends an extracellular filament that traverses the eukaryotic cell membranes to deliver bacterial proteins directly into the host cytoplasm (Costa et al., 2015). Delivered proteins known as effectors target different cellular processes to promote bacterial proliferation and affect host physiological processes to cause

disease (Costa et al., 2015; Buttner, 2016). The T3SS is not constitutively present in the bacterial membrane but its assembly is triggered by the bacterial recognition of the eukaryotic host and its adhesion to it (Costa et al., 2015). Because plant cells are surrounded by a rigid cell wall, the extracellular component of the T3SS in plant pathogenic bacteria also includes a needle extension and the Hrp pilus (He and Jin, 2003).

1.3 The Type Three Secretion System (T3SS) in *P. syringae*

In *P. syringae,* the T3SS is encoded by a set of genes named *hrp/hrc* (hypersensitive response and pathogenicity/hypersensitive response and conserved genes (Collmer et al., 2000). The *hrp/hrc* genes include six operons and are flanked by regions encoding effectors translocated through the T3SS and called "Exchangeable Effector Locus (EEL)" and "Conserved Effector Locus (CEL)" (Alfano et al., 2000). The *hrp/hrc* genes together with the EEL and CEL make the Hrp pathogenicity island, likely acquired through horizontal gene transfer (Alfano et al., 2000). In addition to the effectors encoded in the EEL and CEL, other effectors are located elsewhere in the genome (Alfano et al., 2000). With the availability of genomic sequences for several pathovars of *P. syringae* (Buell et al., 2003; Feil et al., 2005; Joardar et al., 2005; Vinatzer et al., 2006; Almeida et al., 2009; Reinhardt et al., 2009), the entire repertoire of effectors has been unraveled and found to be different among different pathovars. As a species, *P. syringae* encodes 57 families of effectors (Lindeberg et al., 2012), with each pathovar encoding between 15 to 30 effectors that can be unique or broadly conserved among pathovars.

1.4 Effectors from *P. syringae* pv. tomato DC3000 (*Pst* DC3000) Translocated by the T3SS

The genomic sequence of *Pst* DC3000 (Buell et al., 2003) enabled the identification of effectors. Initially the effectors were discovered by examining their promoters and identifying *hrp* regulatory sequences (Zwiesler-Vollick et al., 2002). Further bioinformatics approaches allowed deducing

particular combinations of amino acids at the N-terminus as signatures of T3SS effectors (Petnicki-Ocwieja et al., 2002). These bioinformatics predictions were further validated through *in planta* translocation assays. For such assays putative effectors were cloned as fusions to the calmodulin-dependent adenylate cyclase (Cya) gene that is only produced in eukaryotes. Delivery of these effector-Cya fusions by T3SS-competent bacteria into plants was demonstrated by the production of cyclic AMP (cAMP) (Schechter et al., 2004). Altogether, these approaches led to the identification of at least 28 active effectors, 18 of them located in six different gene clusters and the rest of them spread throughout the *Pst* DC3000 genome (Chang et al., 2005; Schechter et al., 2006).

Pst DC3000 effectors are called Hops (Hrp outer protein) and trigger two distinct responses when injected into plant cells depending on whether the plant is a host or a nonhost (Collmer et al., 2000; Lindeberg et al., 2012). In host plants, bacteria are able to cause disease and translocated effectors promote bacterial parasitism by targeting physiological processes in the plants and by interfering with the plant immune system (Buttner, 2016). In nonhost plants, these effectors are recognized by the plant and trigger the hypersensitive response (HR), a defense associated mechanism of programmed cell death (Balint-Kurti, 2019). In that case the effectors function as avirulence proteins (Avr).

1.5 The Plant Immune System

Similar to animals, plants are endowed with an innate immune system to detect the presence of potential pathogens and prevent their proliferation. This immune system includes preformed physical and chemical barriers, as well as inducible responses that are activated upon pathogen recognition either extracellularly or intracellularly (Senthil-Kumar and Mysore, 2013). Because each plant species is defined by its genetic makeup, their preformed and inducible defenses may or may not protect them from pathogens. This plant species-specific phenomenon is called

"Nonhost resistance" and explains why the majority of plant species are resistant to most pathogens and succumb to disease by only few. Nonhost resistance is broad spectrum, and while all the components of nonhost resistance are still unknown, it has been proposed that nonhost resistance functions at three different levels: preventing pathogen entry, limiting pathogen multiplication, and directly killing the pathogen by secretion of antimicrobials (Senthil-Kumar and Mysore, 2013).

To prevent pathogen entry, plants recognize pathogens through Plant Recognition Receptors (PRRs) located on the surface of plant cells (Zipfel, 2014). The ligands that PRRs recognize are conserved proteins in microbes called "Microbe-Associated Molecular Patterns" (MAMPs), also called "Pathogen-Associated Molecular Patterns" (PAMPs) (Yu et al., 2017), when such microbes are pathogens. MAMPs/PAMPs recognition triggers a cascade of responses including stomatal closure, cell wall strengthening by deposition of callose and lignin, generation of reactive oxygen species (ROS) and phenolic compounds and accumulation of plant hormones (Senthil-Kumar and Mysore, 2013). The collection of responses triggered upon PAMPs recognition by PRRs, has been called PAMP-triggered immunity (PTI) (Jones and Dangl, 2006). PTI is non-specific and prevent the ingress of non-pathogenic microorganisms as well as potentially pathogenic microorganism that are not equipped to cause disease in a particular plant, also known as non-adapted pathogens. In contrast to non-adapted pathogens, adapted pathogens are able to penetrate plant tissues because they are able to interfere with plant responses associated with PTI (Jones and Dangl, 2006).

Although adapted pathogens are able to suppress PTI, some can be recognized by the plant immune system when they deploy particular effectors. Those effectors are recognized intracellular receptors and activate a second layer of immunity called "effector-triggered immunity" (ETI) (Jones and Dangl, 2006). While ETI triggers the same responses as PTI, ETI responses occur

faster and have higher intensity than those activated by PTI (Tao et al., 2003), and culminate with the hypersensitive response (HR), a type of programmed cell death (PCD) that restricts local pathogen growth (Greenberg and Yao, 2004).

1.6 *Pst DC3000* Effectors Target Plant Immune Responses and Plant Physiological Processes

In order to cause disease *Pst* DC3000 deploy several effectors to suppress plant immune responses. For example, AvrPto targets the PRRs FLS2 (flagellin-sensitive 2) and EFR (EF-Tu receptor) that recognize the bacterial PAMPs flagellin (flg22) and the elongation factor EF-Tu, respectively (Gomez-Gomez and Boller, 2000; Kunze et al., 2004; Chinchilla et al., 2007) . Another *Pst*DC3000 effector AvrPtoB targets the CERK1 (chitin elicitor receptor kinase 1) that recognizes chitin and bacterial peptidoglycan (Miya et al., 2007; Gimenez-Ibanez et al., 2009; Willmann et al., 2011). AvrPto and AvrPtoB trigger the degradation of PRRs and by doing so interfere with downstream signaling cascades (Shan et al., 2000).

In addition to AvrPto and AvrPtoB targeting pathogen recognition processes, other *Pst*DC3000 effectors such as: HopD1, HopM1 and HopU1 interfere with the expression of defense related genes (Nomura et al., 2006; Fu et al., 2007; Block et al., 2014; Lozano-Duran et al., 2014) and HopI1 localizes to chloroplast and inhibits the production of salicylic acid (SA), a plant hormone involved in immune responses (Jelenska et al., 2007).

Although the elucidation of the function of *Pst* DC3000 effectors has advanced significantly, the function of many effectors and their host cellular targets are still unknown. This work presents the characterization of two effectors in *Pst* DC3000, HopD1 and HopG1 targeting the plant protein in Arabidopsis named AtNHR2B (*Arabidopsis thaliana* nonhost resistance 2B), a protein

important in nonhost resistance that contributes to the deposition of callose to the cell wall (Singh et al., 2018).

2 References

Alfano, J.R., Charkowski, A.O., Deng, W.L., Badel, J.L., Petnicki-Ocwieja, T., van Dijk, K., and Collmer, A. 2000. The Pseudomonas syringae Hrp pathogenicity island has a tripartite mosaic structure composed of a cluster of type III secretion genes bounded by exchangeable effector and conserved effector loci that contribute to parasitic fitness and pathogenicity in plants. Proceedings of the National Academy of Sciences of the United States of America 97:4856-4861.

Almeida, N.F., Yan, S., Lindeberg, M., Studholme, D.J., Schneider, D.J., Condon, B., Liu, H.J., Viana, C.J., Warren, A., Evans, C., Kemen, E., MacLean, D., Angot, A., Martin, G.B., Jones, J.D., Collmer, A., Setubal, J.C., and Vinatzer, B.A. 2009. A Draft Genome Sequence of Pseudomonas syringae pv. tomato T1 Reveals a Type III Effector Repertoire Significantly Divergent from That of Pseudomonas syringae pv. tomato DC3000. Molecular Plant-Microbe Interactions 22:52-62.

Aragon, I.M., Perez-Martinez, I., Moreno-Perez, A., Cerezo, M., and Ramos, C. 2014. New insights into the role of indole-3-acetic acid in the virulence of Pseudomonas savastanoi pv. savastanoi. Fems Microbiology Letters 356:184-192.

Balint-Kurti, P. 2019. The plant hypersensitive response: concepts, control and consequences. Molecular Plant Pathology 20:1163-1178.

Bender, C.L., Alarcon-Chaidez, F., and Gross, D.C. 1999. Pseudomonas syringae phytotoxins: Mode of action, regulation, and biosynthesis by peptide and polyketide synthetases. Microbiology and Molecular Biology Reviews 63:266-+.

Block, A., Toruno, T.Y., Elowsky, C.G., Zhang, C., Steinbrenner, J., Beynon, J., and Alfano, J.R. 2014. The Pseudomonas syringae type III effector HopD1 suppresses effector-triggered immunity, localizes to the endoplasmic reticulum, and targets the Arabidopsis transcription factor NTL9. New Phytologist 201:1358-1370.

Buell, C.R., Joardar, V., Lindeberg, M., Selengut, J., Paulsen, I.T., Gwinn, M.L., Dodson, R.J., Deboy, R.T., Durkin, A.S., Kolonay, J.F., Madupu, R., Daugherty, S., Brinkac, L., Beanan, M.J., Haft, D.H., Nelson, W.C., Davidsen, T., Zafar, N., Zhou, L.W., Liu, J., Yuan, Q.P., Khouri, H., Fedorova, N., Tran, B., Russell, D., Berry, K., Utterback, T., Van Aken, S.E., Feldblyum, T.V., D'Ascenzo, M., Deng, W.L., Ramos, A.R., Alfano, J.R., Cartinhour, S., Chatterjee, A.K., Delaney, T.P., Lazarowitz, S.G., Martin, G.B., Schneider, D.J., Tang, X.Y., Bender, C.L., White, O., Fraser, C.M., and Collmer, A. 2003. The complete genome sequence of the Arabidopsis and tomato pathogen Pseudomonas syringae pv. tomato DC3000. Proceedings of the National Academy of Sciences of the United States of America 100:10181-10186.

Buttner, D. 2016. Behind the lines-actions of bacterial type III effector proteins in plant cells. Fems Microbiology Reviews 40:894-937.

Chang, J.H., Urbach, J.M., Law, T.F., Arnold, L.W., Hu, A., Gombar, S., Grant, S.R., Ausubel, F.M., and Dangl, J.L. 2005. A high-throughput, near-saturating screen for type III effector genes from Pseudomonas syringae. Proceedings of the National Academy of Sciences of the United States of America 102:2549-2554.

Chinchilla, D., Zipfel, C., Robatzek, S., Kemmerling, B., Nurnberger, T., Jones, J.D.G., Felix, G., and Boller, T. 2007. A flagellin-induced complex of the receptor FLS2 and BAK1 initiates plant defence. Nature 448:497-U412.

Collmer, A., Badel, J.L., Charkowski, A.O., Deng, W.L., Fouts, D.E., Ramos, A.R., Rehm, A.H., Anderson, D.M., Schneewind, O., van Dijk, K., and Alfano, J.R. 2000. Pseudomonas syringae Hrp type III secretion system and effector proteins. Proceedings of the National Academy of Sciences of the United States of America 97:8770-8777.

Costa, T.R.D., Felisberto-Rodrigues, C., Meir, A., Prevost, M.S., Redzej, A., Trokter, M., and Waksman, G. 2015. Secretion systems in Gram-negative bacteria: structural and mechanistic insights. Nature Reviews Microbiology 13:343-359.

Duca, D., Lorv, J., Patten, C.L., Rose, D., and Glick, B.R. 2014. Indole-3-acetic acid in plant-microbe interactions. Antonie Van Leeuwenhoek International Journal of General and Molecular Microbiology 106:85-125.

Feil, H., Feil, W.S., Chain, P., Larimer, F., DiBartolo, G., Copeland, A., Lykidis, A., Trong, S., Nolan, M., Goltsman, E., Thiel, J., Malfatti, S., Loper, J.E., Lapidus, A., Detter, J.C., Land, M., Richardson, P.M., Kyrpides, N.C., Ivanova, N., and Lindow, S.E. 2005. Comparison of the complete genome sequences of Pseudomonas syringae pv. syringae B728a and pv. tomato DC3000. Proceedings of the National Academy of Sciences of the United States of America 102:11064-11069.

Fett, W.F., and Dunn, M.F. 1989. Exopolysaccharides produced by phytopathogenic Pseudomonas syringae pathovars in infected leaves of susceptible hosts. Plant Physiology 89:5-9.

Fu, Z.Q., Guo, M., Jeong, B.R., Tian, F., Elthon, T.E., Cerny, R.L., Staiger, D., and Alfano, J.R. 2007. A type III effector ADP-ribosylates RNA-binding proteins and quells plant immunity. Nature 447:284-U281.

Gardan, L., David, C., Morel, M., Glickmann, E., Abughorrah, M., Petit, A., and Dessaux, Y. 1992. Evidence for a correlation between auxin production and host plant-species among strains of Pseudomonas syringae subsp savastanoi. Applied and Environmental Microbiology 58:1780-1783.

Gimenez-Ibanez, S., Hann, D.R., Ntoukakls, V., Petutschnig, E., Lipka, V., and Rathjen, J.P. 2009. AvrPtoB Targets the LysM Receptor Kinase CERK1 to Promote Bacterial Virulence on Plants. Current Biology 19:423-429.

Glickmann, E., Gardan, L., Jacquet, S., Hussain, S., Elasri, M., Petit, A., and Dessaux, Y. 1998. Auxin production is a common feature of most pathovars of Pseudomonas syringae. Molecular Plant-Microbe Interactions 11:156-162.

Gomez-Gomez, L., and Boller, T. 2000. FLS2: An LRR receptor-like kinase involved in the perception of the bacterial elicitor flagellin in Arabidopsis. Molecular Cell 5:1003-1011.

Greenberg, J.T., and Yao, N. 2004. The role and regulation of programmed cell death in plant-pathogen interactions. Cellular Microbiology 6:201-211.

He, S.Y., and Jin, Q. 2003. The Hrp pilus: learning from flagella. Curr Opin Microbiol 6:15-19.

Howden, A.J.M., Rico, A., Mentlak, T., Miguet, L., and Preston, G.M. 2009. Pseudomonas syringae pv. syringae B728a hydrolyses indole-3-acetonitrile to the plant hormone indole-3-acetic acid. Molecular Plant Pathology 10:857-865.

Jelenska, J., Yao, N., Vinatzer, B.A., Wright, C.M., Brodsky, J.L., and Greenberg, J.T. 2007. A J domain virulence effector of Pseudomonas syringae remodels host chloroplasts and suppresses defenses. Current Biology 17:499-508.

Joardar, V., Lindeberg, M., Jackson, R.W., Selengut, J., Dodson, R., Brinkac, L.M., Daugherty, S.C., DeBoy, R., Durkin, A.S., Giglio, M.G., Madupu, R., Nelson, W.C., Rosovitz, M.J., Sullivan, S., Crabtree, J., Creasy, T., Davidsen, T., Haft, D.H., Zafar, N., Zhou, L.W., Halpin, R., Holley, T., Khouri, H., Feldblyum, T., White, O., Fraser, C.M., Chatterjee, A.K., Cartinhour, S., Schneider, D.J., Mansfield, J., Collmer, A., and Buell, C.R. 2005. Whole-genome sequence analysis of Pseudomonas syringae pv. phaseolicola 1448A reveals divergence among pathovars in genes involved in virulence and transposition. Journal of Bacteriology 187:6488-6498.

Jones, J.D.G., and Dangl, J.L. 2006. The plant immune system. Nature 444:323-329.

Keith, R.C., Keith, L.M.W., Hernandez-Guzman, G., Uppalapati, S.R., and Bender, C.L. 2003. Alginate gene expression by Pseudomonas syringae pv. tomato DC3000 in host and non-host plants. Microbiology-Sgm 149:1127-1138.

Kunze, G., Zipfel, C., Robatzek, S., Niehaus, K., Boller, T., and Felix, G. 2004. The N terminus of bacterial elongation factor Tu elicits innate immunity in Arabidopsis plants. Plant Cell 16:3496-3507.

Laue, H., Schenk, A., Li, H., Lambertsen, L., Neu, T.R., Molin, S., and Ullrich, M.S. 2006. Contribution of alginate and levan production to biofilm formation by Pseudomonas syringae. Microbiology-Sgm 152:2909-2918.

Lindeberg, M., Cunnac, S., and Collmer, A. 2012. Pseudomonas syringae type III effector repertoires: last words in endless arguments. Trends Microbiol 20:199-208.

Lozano-Duran, R., Bourdais, G., He, S.Y., and Robatzek, S. 2014. The bacterial effector HopM1 suppresses PAMP-triggered oxidative burst and stomatal immunity. New Phytologist 202:259-269.

Mansfield, J., Genin, S., Magori, S., Citovsky, V., Sriariyanum, M., Ronald, P., Dow, M., Verdier, V., Beer, S.V., Machado, M.A., Toth, I., Salmond, G., and Foster, G.D. 2012. Top 10 plant pathogenic bacteria in molecular plant pathology. Molecular Plant Pathology 13:614-629.

McClerklin, S.A., Lee, S.G., Harper, C.P., Nwumeh, R., Jez, J.M., and Kunkel, B.N. 2018. Indole-3-acetaldehyde dehydrogenase-dependent auxin synthesis contributes to virulence of Pseudomonas syringae strain DC3000. PLoS Pathog 14:e1006811.

Melotto, M., Underwood, W., and He, S.Y. 2008. Role of Stomata in Plant Innate Immunity and Foliar Bacterial Diseases. Annu Rev Phytopathol 46:101-122.

Miya, A., Albert, P., Shinya, T., Desaki, Y., Ichimura, K., Shirasu, K., Narusaka, Y., Kawakami, N., Kaku, H., and Shibuya, N. 2007. CERK1, a LysM receptor kinase, is essential for chitin elicitor signaling in Arabidopsis. Proceedings of the National Academy of Sciences of the United States of America 104:19613-19618.

Mutka, A.M., Fawley, S., Tsao, T., and Kunkel, B.N. 2013. Auxin promotes susceptibility to Pseudomonas syringae via a mechanism independent of suppression of salicylic acid-mediated defenses. Plant Journal 74:746-754.

Nomura, K., Debroy, S., Lee, Y.H., Pumplin, N., Jones, J., and He, S.Y. 2006. A bacterial virulence protein suppresses host innate immunity to cause plant disease. Science 313:220-223.

Petnicki-Ocwieja, T., Schneider, D.J., Tam, V.C., Chancey, S.T., Shan, L., Jamir, Y., Schechter, L.M., Janes, M.D., Buell, C.R., Tang, X.Y., Collmer, A., and Alfano, J.R. 2002. Genomewide identification of proteins secreted by the Hrp type III protein secretion system of Pseudomonas syringae pv. tomato DC3000. Proceedings of the National Academy of Sciences of the United States of America 99:7652-7657.

Reinhardt, J.A., Baltrus, D.A., Nishimura, M.T., Jeck, W.R., Jones, C.D., and Dangl, J.L. 2009. De novo assembly using low-coverage short read sequence data from the rice pathogen Pseudomonas syringae pv. oryzae. Genome Research 19:294-305.

Schechter, L.M., Roberts, K.A., Jamir, Y., Alfano, J.R., and Collmer, A. 2004. Pseudomonas sytingae type III secretion system targeting signals and novel effectors studied with a Cya translocation reporter. Journal of Bacteriology 186:543-555.

Schechter, L.M., Vencato, M., Jordan, K.L., Schneider, S.E., Schneider, D.J., and Collmer, A. 2006. Multiple approaches to a complete inventory of Pseudomonas syringae pv. tomato DC3000 type III secretion system effector proteins. Molecular Plant-Microbe Interactions 19:1180-1192.

Senthil-Kumar, M., and Mysore, K.S. 2013. Nonhost Resistance Against Bacterial Pathogens: Retrospectives and Prospects. Pages 407-+ in: Annual Review of Phytopathology, Vol 51, N.K. VanAlfen, ed. Annual Reviews, Palo Alto.

Shan, L.B., Thara, V.K., Martin, G.B., Zhou, J.M., and Tang, X.Y. 2000. The pseudomonas AvrPto protein is differentially recognized by tomato and tobacco and is localized to the plant plasma membrane. Plant Cell 12:2323-2337.

Singh, R., Lee, S., Ortega, L., Ramu, V.S., Senthil-Kumar, M., Blancaflor, E.B., Rojas, C.M., and Mysore, K.S. 2018. Two Chloroplast-Localized Proteins: AtNHR2A and AtNHR2B, Contribute to Callose Deposition During Nonhost Disease Resistance in Arabidopsis. Mol Plant Microbe Interact 31:1280-1290.

Tao, Y., Xie, Z.Y., Chen, W.Q., Glazebrook, J., Chang, H.S., Han, B., Zhu, T., Zou, G.Z., and Katagiri, F. 2003. Quantitative nature of Arabidopsis responses during compatible and incompatible interactions with the bacterial pathogen Pseudomonas syringae. Plant Cell 15:317-330.

Vinatzer, B.A., Teitzel, G.M., Lee, M.W., Jelenska, J., Hotton, S., Fairfax, K., Jenrette, J., and Greenberg, J.T. 2006. The type III effector repertoire of Pseudomonas syringae pv. syringae B728a and its role in survival and disease on host and non-host plants. Molecular Microbiology 62:26-44.

Willmann, R., Lajunen, H.M., Erbs, G., Newman, M.A., Kolb, D., Tsuda, K., Katagiri, F., Fliegmann, J., Bono, J.J., Cullimore, J.V., Jehle, A.K., Gotz, F., Kulik, A., Molinaro, A., Lipka, V., Gust, A.A., and Nurnberger, T. 2011. Arabidopsis lysin-motif proteins LYM1 LYM3 CERK1 mediate bacterial peptidoglycan sensing and immunity to bacterial infection. Proceedings of the National Academy of Sciences of the United States of America 108:19824-19829.

Xin, X.F., Kvitko, B., and He, S.Y. 2018. Pseudomonas syringae: what it takes to be a pathogen. Nature Reviews Microbiology 16:316-328.

Yu, X., Feng, B.M., He, P., and Shan, L.B. 2017. From Chaos to Harmony: Responses and Signaling upon Microbial Pattern Recognition. Pages 109-137 in: Annual Review of Phytopathology, Vol 55, J.E. Leach and S.E. Lindow, eds. Annual Reviews, Palo Alto.

Zipfel, C. 2014. Plant pattern-recognition receptors. Trends in Immunology 35:345-351.

Zwiesler-Vollick, J., Plovanich-Jones, A.E., Nomura, K., Bandyopadhyay, S., Joardar, V., Kunkel, B.N., and He, S.Y. 2002. Identification of novel hrp-regulated genes through functional genomic analysis of the Pseudomonas syringae pv. tomato DC3000 genome. Molecular Microbiology 45:1207-1218.

3 HopG1 *a Pseudomonas syringae* pv. tomato DC3000 Effector Targets the *Arabidopsis thaliana* Nonhost Resistance 2B (AtNHR2B) Protein

3.1 Introduction

Pseudomonas syringae is a plant pathogenic Gram-negative bacterium that causes disease in a wide range of plants. *P. syringae* species has been divided into more than 50 pathovars based on the host plants they are able to infect (Xin et al., 2018). *Pseudomonas syringae* pv. tomato DC3000 (*Pst* DC3000), the causal agent of bacterial speck on tomato has become a model to understand bacterial pathogenicity and plant-microbe interactions because it also causes disease in the model plant *Arabidopsis thaliana* (Xin and He, 2013). The pathogenicity of *Pst* DC3000 is mostly due to the type III secretion system (T3SS), a complex of proteins spanning the inner and outer bacterial membranes that is attached to an extracellular tubular structure, known as the Hrp pilus (Roine et al., 1997). *Pst* DC3000 uses the T3SS apparatus to deliver bacterial proteins, known as effectors, directly into the host cytoplasm (Lindeberg et al., 2012). The availability of *Pst* DC3000 genomic sequence combined with bio-informatics and experimental approaches have enabled the identification of at least 29 active effectors deployed by this strain (Petnicki-Ocwieja et al., 2002; Lindeberg et al., 2006; Schechter et al., 2006). Several of those effectors have been characterized and shown to interfere with plant defense responses and other physiological processes (Macho, 2016). One of those effectors that has been investigated is HopG1.

HopG1 interferes with Pathogen-Associated Molecular Patters (PAMP)-triggered immunity (PTI) (Jones and Dangl, 2006), one of the tiers of plant immunity. Specifically, transgenic expression of *HopG1* suppresses PTI-mediated callose deposition triggered by inoculation with the *Pst* DC000 *hrcC* mutant defective in the T3SS and therefore considered non-pathogenic (Block et al., 2010). As a consequence of PTI suppression, these transgenic plants supported growth of the *Pst*

DC3000 *hrcC* mutant that is unable to grow in wild-type Col-0 plants (Block et al., 2010). HopG1 localizes to mitochondria (Block et al., 2010) where it interacts with the kinesin motor protein (Shimono et al., 2016).

The present study shows that HopG1 also interacts with AtNHR2B (*Arabidopsis thaliana* nonhost resistance 2B), a protein that is involved in nonhost resistance, a broad-spectrum mechanism that protects plants against the majority of plant pathogens (Singh et al., 2018). Here, *HopG1*-transgenic plants showed enhanced cell death after inoculation with the non-adapted pathogen *P. syringae* pv. tabaci (*Pstab*). The observed cell death was directly related to higher ion leakage and higher accumulation of reactive oxygen species (ROS) in those plants in comparison with wild-type Col-0. Those responses prevented proliferation of *Pstab*. Interestingly, overexpression of *AtNHR2B* in the presence of *HopG1* attenuated these responses and promoted *Pstab* virulence in *Arabidopsis* suggesting that AtNHR2B is a virulence target of HopG1.

3.2 Methods

3.2.1 Bacterial Strains

Wild-type *P. syringae* pv tabaci (*Pstab*) *and Pst* DC3000 were grown on King's B (KB) medium supplemented with rifampicin (25 µg/mL) and grown at 28^{o}C.

Agrobacterium tumefaciens strains were grown at 28°C in Luria-Bertani (LB) medium supplemented with corresponding antibiotics.

3.2.2 Plant Materials and Growth Conditions

A. thaliana seeds were planted in soil and grown for five weeks in a growth chamber at 21 °C with an 8/16 h light/dark cycles. *N. benthamiana* plants were planted in soil and grown for 4 weeks under growth chamber conditions at 25° C with a 10/14 h light/dark cycle.

Transgenic lines expressing *HopG1-FLAG* under the expression of the glucocorticoid promoter were obtained from Dr. Jim Alfano (University of Nebraska, Lincoln). *HopG1-FLAG* plants were transformed with *AtNHR2B-GFP* using floral dip (Clough and Bent, 1998) to generate *AtNHR2B-GFP/HopG1-FLAG* transgenic lines.

For bacterial growth curves and symptoms assessment in *A. thaliana*, plants were grown in Murashige and Skoog (MS) media supplemented with 1µM dexamethasone for two weeks and then transplanted to soil and grown for additional four weeks. For Reactive Oxygen Species (ROS) quantification, ion leakage and trypan blue experiments, plants were grown in soil and sprayed with a 1 µM dexamethasone solution supplemented with 0.01% silwet, 12 hours before inoculation.

3.2.3 Yeast-two Hybrid Assay

To generate constructs for the yeast two-hybrid assay, full length *AtNHR2B* in the entry vector *pDONR201* (provided by Dr. Raksha Singh) was transferred by an LR reaction to the bait vector pDEST32 to generate a fusion to the *GAL4* DNA-binding domain. Full length *HopG1* in the entry vector pENTR/SD/Topo (provided by Dr. Alan Collmer, Cornell University) was transferred by an LR reaction to the prey vector *pDEST22* to generate a fusion to the transcriptional activation domain. The reciprocal clones were also generated wherein *AtNHR2B* was cloned in *pDEST22,* while *HopG1* was cloned into *pDEST32*.

Mav203 yeast cells were transformed using the Frozen-EZ Yeast Transformation II Kit (Zymo Research) with the following combinations of constructs: *pDEST32*::*AtNHR2B* + *pDEST22*::*HopG1*; *pDEST32*::*AtNHR2B* + *pDEST22*; *pDEST32*::*HopG1* + *pDEST22*::*AtNHR2B*; *pDEST32*::*HopG1* + *pDEST22* and *pDEST32* + *pDEST22*::*AtNHR2B*. Transformed yeast cells were plated on Double Drop Out (DDO) selection plates lacking amino acids leucine and tryptophan and grown at 30°C for 4 days. Single colonies were picked from the plates and cultured

in 15 mL DDO broth at 30°C overnight. The overnight culture was diluted to an OD_{600}nm of 0.2 and plated on Triple Drop Out (TDO) selection plates lacking amino acids leucine, tryptophan and histidine supplemented with 15 mM 3-Amino-1,2,4-Triazole (3-AT) and grown at at 30°C for 4 days.

3.2.4 Biomolecular Fluorescence Complementation (BiFC)

To generate the constructs for BiFC, full length *AtNHR2B* and the truncated version *AtNHR2B*$_{1-417}$ in entry vector *pDONR201* were cloned into pSITEnEYFP (Martin et al., 2009) using Gateway Technology, to generate a N-terminal fusion to the N-terminal half of the enhanced yellow fluorescence protein (EYFP). *HopG1* was cloned into pSITEcEYFP to generate an N-terminal fusion to the C-terminal half of EYFP. *pSITE-nEYFP::AtNHR2B, pSITE-nEYFP:: AtNHR2B*$_{1-417}$ and *pSITE-cEYFP*$_{::}$*HopG1* were individually transformed into *A. tumefaciens. A. tumefaciens* strains harboring these constructs were grown overnight, and overnight cultures were centrifuged at 6,000 rpm for 10 minutes. Culture supernatants were discarded and bacterial pellets were re-suspended in induction buffer (20mM MES pH 5.5; 3% sucrose, 200µM acetosyringone) and incubated with constant shaking at room temperature for 4h. Each one of the *A. tumefaciens* strains harboring fusions to the N-terminal half of EYFP and C-terminal half of EYFP were adjusted to an OD_{600} = 0.6, and different combinations of constructs containing fusions to the N-terminal half of EYFP and C-terminal fusions to the EYFP were co-infiltrated into four-week-old *N. benthamiana* plants.

An *A. tumefaciens* strain harboring *pSITE-nEYFP::JAZ1* was co-infiltrated into *N. benthamiana* with *A. tumefaciens* harboring *pSITE-cEYFP*$_{::}$*HopG1* as negative control. After 3 dpi, leaves were collected for live-cell imaging by laser scanning confocal microscopy using excitation wavelength of 514 nm and an emission wavelength of 500 to 530 nm.

3.2.5 Bacterial Growth Curves and Symptoms Assessment in *A. thaliana*

Five-week old wild-type Col-0, *AtNHR2B-GFP*, *HopG1-FLAG* and /*AtNHR2B-GFP*/*HopG1-FLAG* plants were syringe-inoculated with *Pstab* at 1 X 10^7 CFU/mL. At 0 and 3 dpi, four to six inoculated leaves were collected and 0.5 cm^2 disks were cut out using a core-borer, for a total of eight leaf disks per genotype to generate four replicates, each replicate containing two leaf disks. Leaf disks were transferred to 1.7 ml microcentrifuge tubes containing 100 µl ddH_2O and ground. Homogenized tissue was serially diluted and plated on KB agar to enumerate bacterial populations. Each experiment was repeated three times. Symptoms were evaluated at 3 and 6 dpi.

3.2.6 Callose Deposition

Five-week old wild-type Col-0, *AtNHR2B-GFP*, *HopG1-FLAG* and *HopG1-FLAG*/*AtNHR2B-GFP* were inoculated with with *Pstab* at 1 X 10^7 CFU/mL. Six to nine leaves from six independent plants for each genotype and inoculated with *Pstab* or infiltrated with water were detached after 24 hpi and stained with 5% aniline blue to visualize callose deposits (Kvitko et al., 2009). Images were taken by Nikon 90i upright scanning laser confocal microscope (Nikon) using a DAPI (4',6-diamidino-2-phenylindole) filter with excitation wavelength of 405 nm and an emission wavelength of 450-510 nm.

3.2.7 Trypan Blue Staining

Five-week old wild-type Col-0, *AtNHR2B-GFP*, *HopG1-FLAG* and *AtNHR2B-GFP*/*HopG1-FLAG* plants were syringe-inoculated with *Pstab* at OD_{600}=0.02 (1 X 10^6 CFU/mL). Control plants were inoculated with water only. At 24 hpi, six to 9 inoculated leaves were detached from six independent plants for each genotype and stained with 0.05% trypan blue. Images were taken on a light microscope using bright field.

3.2.8 Ion Leakage

Five-week old wild-type Col-0, *AtNHR2B-GFP*, *HopG1-FLAG* and *AtNHR2B-GFP*/*HopG1-FLAG* plants were syringe-inoculated with *Pstab* at OD_{600}=0.02 (1 X 10^6 CFU/mL). Control plants were inoculated with water only. Leaf samples were collected at 24 hpi and leaf disks were cut out using a 0.5 cm^2 core-borer. A total of six disk were collected per genotype to generate three replicates, two leaf disks per replicate. Collected tissue was placed in a 50 mL falcon tube with 15 mL of ddH_2O. Conductivity was measured using the Orion Star A215 conductivity cell (013005MD) (Thermo Fisher Scientific), immediately after placing the samples in water, and three hours after sample incubation with constant shaking at room temperature.

3.2.9 Mitochondrial ROS Production

Five- week old wild-type Col-0, *AtNHR2B-GFP*, *HopG1-FLAG* and *AtNHR2B-GFP*/*HopG1-FLAG* plants grown on soil were used to collect leaf disks cut out using a 1.2 cm core-borer. Harvested tissue was transferred to clear bottom plates for fluorometric analysis and submerged in *Pstab* inoculum at a final concentration of 1 X 10^7 CFU/mL. For mock-treatment, plants were submerged in water. Two hours after inoculation with either *Pstab* mock-treatment, MitoTracker Red CM-H_2XRos (ThermoFisher Scientific) was added at a final concentration of 0.005 mM and incubated for ten minutes before taking the first reading. Fluorescence was measured with an excitation wavelength of 570 nm and an emission wavelength of 535 nm on BioTek luminescence microplate reader.

3.3 Results

3.3.1 The *Pst* DC3000 Effector HopG1 Interacts with *Arabidopsis* Protein AtNHR2B in Yeast and *in Planta*.

Previous findings from the Rojas lab showed that AtNHR2B interacts with proteins localized to the mitochondria (Singh et al, under revision), indirectly implying that AtNHR2B also has

mitochondrial localization. The possible localization of AtNHR2B to the mitochondria led to the hypothesis that AtNHR2B interacted with HopG1, an effector previously shown to be localized to mitochondria (Block et al., 2010; Shimono et al., 2016). This hypothesis was tested initially using the yeast two-hybrid system by co-transforming yeast with *pDEST32::AtNHR2B* and *pDEST22::HopG1*. As control, yeast was also transformed with *pDEST32::AtNHR2B* and empty vector *pDEST22.* Yeast transformed with *pDEST32::AtNHR2B* and *pDEST22::HopG1* grew in TDO. However, yeast transformed with *pDEST32::AtNHR2B* and empty *pDEST22,* also grew in TDO supplemented with 3-AT, indicating auto-activation activity (Figure 1). To circumvent this problem, the reciprocal constructs: *pDEST22::AtNHR2B* and *pDEST32::HopG1* were generated and used for yeast transformation (Figure 1). Yeast co-transformed with *pDEST22::AtNHR2B* and empty *pDEST32* did not cause auto-activation. Yeast co-transformed with the combinations *pDEST22::AtNHR2B* and *pDEST32::HopG1* grew in TDO + 3-AT (Figure 1).

To validate the physical interaction observed in yeast, the AtNHR2B-HopG1 interaction was also evaluated *in- planta* by bimolecular fluorescence complementation (BiFC) after transiently co-expressing AtNHR2B fused to the N-terminal half of EYFP with HopG1 fused to the C-terminal half of EYFP in *N. benthamiana*. A truncated version of AtNHR2B ($AtNHR2B_{1-417}$) fused to the N-terminal half of EYFP was also generated to be used as a potential negative control. JAZ1, a transcriptional repressor involved in jasmonate signaling (Chini et al., 2007) was also fused to the N-terminal half of EYFP to be used as negative control. Full length AtNHR2B, the truncated version $AtNHR2B_{1-417}$ and JAZ1 fused to the N-terminal half of EYFP were co-infiltrated with HopG1 fused to the C-terminal half of EYFP into *N. benthamiana.* Full length AtNHR2B and the truncated version $AtNHR2B_{1-417}$ interacted with HopG1 as observed by the reconstitution of the yellow fluorescence and this interaction in the cytoplasm where AtNHR2B can be localized (Singh et al., 2018). HopG1 does not interact with JAZ1 another plant protein used as negative control (Figure 2). Altogether, these data show that the physical interaction between AtNHR2B and

HopG1 is biologically relevant as it also occurs in planta and further shows that the N-terminal region of AtNHR2B is sufficient for that interaction.

3.3.2 HopG1 Interferes with AtNHR2B Function to Promote Disease

The findings that HopG1 interacts with AtNHR2B in yeast and *in planta* prompted further investigations to dissect the function of HopG1, with the hypothesis that HopG1 interferes with the function of AtNHR2B. To test this hypothesis, transgenic *Arabidopsis* lines expressing *HopG1-FLAG* alone or in combination with *AtNHR2B-GFP* were inoculated with *Pstab*. As a non-adapted pathogen of *Arabidopsis*, *Pstab* is unable to cause disease in wild-type Col-0 plants. In these experiments, *Pstab* did not cause disease symptoms in wild-type Col-0 plants, nor in transgenic plants expressing *AtNHR2B-GFP* (Figure 3A). Consistently with this result, *Pstab* did not grow and bacterial populations at 3 dpi were not significantly higher than those at 0 dpi. Interestingly, inoculation of *Pstab* in transgenic plants expressing *HopG1-Flag* had different phenotypes. Transgenic plants expressing *HopG1-FLAG* alone showed no disease symptoms, only localized death around the site of inoculation reminiscent of the hypersensitive response (HR) (Figure 3A). In these plants, *Pstab* populations were not significantly different than *Pstab* populations in wild-type Col-0 (Figure 3B). However, *Pstab* inoculation on plants co-expressing *HopG1-FLAG* with *AtNHR2B-GFP* caused disease symptoms characterized by extensive tissue damage with chlorotic patches close to the inoculation site, as well as close to the leave petiole (Figure 3A) and 10-fold increase in bacterial growth (Figure 3B), indicating that the combination of *HopG1* and overexpression of *AtNHR2B* enhances susceptibility to disease.

3.3.3 HopG1 Suppresses Callose Deposition

The findings that AtNHR2B is important with the deposition of callose (Singh et al., 2018), together with the findings that HopG1 interacts with AtNHR2B, led to the hypothesis that HopG1 interferes

with callose deposition. To test this hypothesis wild-type Col-0, and the transgenic lines *AtNHR2B-GFP*, *HopG1-FLAG* and *AtNHR2B-GFP/HopG1-FLAG* were inoculated with *Pstab* or mock-treated with water, and inoculated leaves were stained with aniline blue to evaluate callose deposits. Wild-type Col-0 along with transgenic plants overexpressing AtNHR2B-GFP, exhibited abundant callose deposits in response to bacterial inoculation (Figure 4). In contrast, *Arabidopsis* plants expressing the bacterial effector *HopG1-FLAG* alone or in combination with *AtNHR2B-GFP* showed deficiency in depositing callose (Figure 4), demonstrating that HopG1 interferes with callose deposition and it is able to do so even when *AtNHR2B-GFP* is overexpressed.

3.3.4 HopG1 Promotes Cell Death after Inoculation with a Non-adapted Pathogen

The finding that transgenic expression of *HopG1-FLAG* alone triggered cell death prompted further investigations into cell death phenotypes and, for that purpose, plants inoculated with *Pstab* or mock-treated were further stained with trypan blue to evaluate cell viability. Mock-treated plants did not uptake the trypan blue stain demonstrating that the cells are alive. Similar results were obtained with wild-type Col-0 and *AtNHR2B-GFP*-transgenic plants inoculated with *Pstab*. However, dramatic cell death visualized by extensive uptake of the trypan blue dye, was observed in transgenic plants expressing *HopG1-FLAG* alone. Surprisingly, transgenic plants co-expressing *HopG1-FLAG* with *AtNHR2B-GFP* and inoculated with *Pstab* also showed cell death but the levels of cell death were reduced in comparison with those in *HopG1-FLAG* plants (Figure 5). These results indicate that HopG1 causes cell death upon infection with *Pstab* but the extend of the cell death is controlled by the presence of AtNHR2B.

To provide a quantitative measurement for the cell death phenotypes observed, ion leakage was examined in wild-type Col-0, and in transgenic plants expressing *HopG1-FLAG, ANHR2B-GFP* and *AtNHR2B-GFP/HopG1-FLAG* after mock treatment, and after inoculation with *Pstab.*

Conductivity readings associated with ion leakage showed that mock- treated plants had low levels of conductivity as expected, considering they did not have cell death. Wild-type Col-0 plants inoculated with *Pstab* showed significantly higher levels of ion leakage in comparison with mock-treated plants. *AtNHR2B*-GFP-expressing plants as well as plants co-expressing *HopG1-FLAG* and *AtNHR2B-GFP* had moderate levels of ion leakage. The highest levels of ion leakage were observed in plants expressing *HopG1-FLAG* alone, consistent with the extended cell death phenotype observed in these plants (Figure 6).

3.3.5 HopG1 Regulates Production of ROS in the Mitochondria

Because cell death phenotypes are regulated by reactive oxygen species (ROS), and mitochondria are the source of ROS, it was necessary to evaluate whether HopG1 contributes to the production of ROS in the mitochondria. For that purpose, a mitochondria-specific ROS sensor was used to evaluate mitochondrial ROS produced after pathogen infection. Inoculation of *Pstab* triggered an accumulation of mitochondrial ROS in all the plants. However, the levels of accumulation varied. The lowest levels of mitochondrial ROS were observed in wild-type Col-0, moderate levels were found in transgenic plants expressing *AtNHR2B-GFP* and co-expressing *HopG1-Flag* and *AtNH2B-GFP.* The highest levels of mitochondrial ROS were observed in plants expressing *HopG1-Flag* alone (Figure 7).

3.4 Discussion

This study unraveled a new function for HopG1 targeting AtNHR2B, a plant protein that was identified as a component of nonhost resistance (Singh et al., 2018). The evidence that HopG1 targets AtNHR2B includes protein-protein interaction assays demonstrating physical interaction between HopG1 and AtNHR2B in yeast and *in planta,* as well as genetic data using transgenic plants expressing *HopG1* alone, or in combination with *AtNHR2B.*

HopG1 has been considered a suppressor of defense responses based on studies using *N. benthamiana.* In such studies, inoculating the *Pst* DC3000 *hopG1* mutant into *N. benthamiana* caused the HR, while inoculating the *Pst* DC3000 *hopG1* (*pHopG1*) complementing strain did not cause an HR (Jamir et al., 2004). Similarly, a *Pst* DC3000 strain deleted of all effectors and only harboring HopG*1* failed to elicit cell death in *N. benthamiana* (Wei et al., 2018). Furthermore, transient expression of the cell death inducer *BAX1* (Baek et al., 2004) in *N. benthamiana* triggered the HR as expected, but this HR was not observed when *BAX1* was transiently co-expressed with *HopG1* (Jamir et al., 2004). While these observations provided insight into the function of *HopG1,* they should not be considered generalization for all plants.

In *Arabidopsis,* the function of HopG1 has also been investigated generating transgenic plants expressing this effector. The use of transgenic plants expressing bacterial effectors is a common approach to interrogate effector function without the confounding effects associated with the inherent redundancy of effectors and the interplay among them (Wilton and Desveaux, 2010). Indeed, transgenic plants expressing the effectors *AvrB*, *AvrRpt2, HopF2* and HopAI1 have been instrumental into gaining insight into their respective functions in plant immunity (Gopalan et al., 1996; Chen et al., 2000; Zhang et al., 2007; Wilton et al., 2010). Transgenic plants constitutively expressing *HopG1* showed reduced callose deposition upon treatment with the PTI triggering peptide Flg21 and after infiltration with the non-pathogenic bacterium *Pseudomonas fluorescens* (Block et al., 2010). Moreover, *HopG1*-expressing plants supported higher growth of the *Pst* DC3000 *hrcC* mutant in comparison with its growth in wild-type Col-0 (Block et al., 2010). Because the *Pst* DC3000 *hrcC* mutant is defective in T3SS, it behaves like a non-pathogen when inoculated into any plant. Thus, inoculation of the *Pst* DC3000 *hrcC* into *Arabidopsis* is used to evaluate activation of PTI (Block et al., 2010). This activation of PTI is expected to also occur with *Pstab* as this bacterium is not equipped to cause disease in *Arabidopsis.* This work shows that

HopG1-expression suppresses callose deposition in response to *Pstab* in agreement with previously published results (Block et al., 2010).

However, in contrast with those published results, this study showed that the growth of *Pstab* in *HopG1-FLAG* transgenic plants is not different from its growth in wild-type Col-0. Therefore, transgenic expression of *HopG1-FLAG* does not suppress plant defense responses as previously reported (Block et al., 2010). Actually, this study presents compelling evidence that transgenic expression of *HopG1* induces cell death in response to inoculation with *Pstab.* Moreover, that cell death, observed by trypan blue staining and quantification of ion leakage, is a defense response as *HopG1-FLAG*- expressing plants did not develop disease symptoms nor supported higher bacterial growth in comparison with wild-type Col-0 plants. All these results demonstrate that *HopG1* triggers a bona-fide HR.

The previous study, also showed that *HopG1*-transgenic plants had increased accumulation of ROS (Block et al., 2010). However, that study used the ROS sensitive probe H2DCFDA (2'-7'-dichlorodihydrofluorescein), that does not discriminate among the multiple sources of ROS. This study more precisely defined that the higher levels of ROS in *HopG1*-transgenic lines are from mitochondrial origin, which are in line with the mitochondrial localization of HopG1. These results suggest that *HopG1* expression and localization to mitochondria (Block et al., 2010) actually induces the production of mitochondrial ROS that likely activate a cell death program. In that context, HopG1 appears to act as an avirulence effector. Interestingly, the *HopG1*-mediated cell death is attenuated when *AtNHR2B* is overexpressed. Plants co-expressing *HopG1-FLAG* and *AtNHR2B-GFP* showed conspicuous symptoms characterized by extended lesions with chlorotic spots, enhanced bacterial growth, reduced cell death and reduced accumulation of ROS. These results agree with other studies showing that *Pst* DC300 type III effectors need its plant target to promote bacterial virulence. For example, HopF2 targets the plant protein RIN4 to promote

virulence (Wilton et al., 2010). It is possible that the overexpression of *AtNHR2B* makes it a virulence target for HopG1, and that when this plant protein is not being overexpressed, HopG1 is recognized by an unknown mechanism and that mechanism triggers the HR that prevents the onset of disease symptoms and limits bacterial proliferation.

The results from this work showed that HopG1 might function at two stages: at early stages, HopG1 can suppress callose deposition triggered by the non-specific recognition mechanism, and at later stages can function in avirulence determinant that triggers an HR associated with the mitochondrial production of ROS. In the presence of AtNHR2B, HopG1 acquires virulence functions.

3.5 References

Baek, D., Nam, J., Koo, Y.D., Kim, D.H., Lee, J., Jeong, J.C., Kwak, S.S., Chung, W.S., Lim, C.O., Bahk, J.D., Hong, J.C., Lee, S.Y., Kawai-Yamada, M., Uchimiya, H., and Yun, D.J. 2004. Bax-induced cell death of Arabidopsis is meditated through reactive oxygen-dependent and -independent processes. Plant Mol Biol 56:15-27.

Block, A., Guo, M., Li, G.Y., Elowsky, C., Clemente, T.E., and Alfano, J.R. 2010. The Pseudomonas syringae type III effector HopG1 targets mitochondria, alters plant development and suppresses plant innate immunity. Cellular Microbiology 12:318-330.

Chen, Z., Kloek, A.P., Boch, J., Katagiri, F., and Kunkel, B.N. 2000. The Pseudomonas syringae avrRpt2 gene product promotes pathogen virulence from inside plant cells. Mol Plant Microbe Interact 13:1312-1321.

Chini, A., Fonseca, S., Fernandez, G., Adie, B., Chico, J.M., Lorenzo, O., Garcia-Casado, G., Lopez-Vidriero, I., Lozano, F.M., Ponce, M.R., Micol, J.L., and Solano, R. 2007. The JAZ family of repressors is the missing link in jasmonate signalling. Nature 448:666-671.

Clough, S.J., and Bent, A.F. 1998. Floral dip: a simplified method for Agrobacterium-mediated transformation of Arabidopsis thaliana. Plant J 16:735-743.

Gopalan, S., Bauer, D.W., Alfano, J.R., Loniello, A.O., He, S.Y., and Collmer, A. 1996. Expression of the Pseudomonas syringae avirulence protein AvrB in plant cells alleviates its dependence on the hypersensitive response and pathogenicity (Hrp) secretion system in eliciting genotype-specific hypersensitive cell death. Plant Cell 8:1095-1105.

Jamir, Y., Guo, M., Oh, H.S., Petnicki-Ocwieja, T., Chen, S., Tang, X., Dickman, M.B., Collmer, A., and Alfano, J.R. 2004. Identification of Pseudomonas syringae type III effectors that can suppress programmed cell death in plants and yeast. Plant J 37:554-565.

Jones, J.D., and Dangl, J.L. 2006. The plant immune system. Nature 444:323-329.

Kvitko, B.H., Park, D.H., Velasquez, A.C., Wei, C.F., Russell, A.B., Martin, G.B., Schneider, D.J., and Collmer, A. 2009. Deletions in the Repertoire of Pseudomonas syringae pv. tomato DC3000 Type III Secretion Effector Genes Reveal Functional Overlap among Effectors. Plos Pathogens 5:16.

Lindeberg, M., Cunnac, S., and Collmer, A. 2012. Pseudomonas syringae type III effector repertoires: last words in endless arguments. Trends Microbiol 20:199-208.

Lindeberg, M., Cartinhour, S., Myers, C.R., Schechter, L.M., Schneider, D.J., and Collmer, A. 2006. Closing the circle on the discovery of genes encoding Hrp regulon members and type III secretion system effectors in the genomes of three model Pseudomonas syringae strains. Molecular plant-microbe interactions : MPMI 19:1151-1158.

Macho, A.P. 2016. Subversion of plant cellular functions by bacterial type-III effectors: beyond suppression of immunity. New Phytol 210:51-57.

Martin, K., Kopperud, K., Chakrabarty, R., Banerjee, R., Brooks, R., and Goodin, M.M. 2009. Transient expression in Nicotiana benthamiana fluorescent marker lines provides enhanced definition of protein localization, movement and interactions in planta. Plant J 59:150-162.

Petnicki-Ocwieja, T., Schneider, D.J., Tam, V.C., Chancey, S.T., Shan, L., Jamir, Y., Schechter, L.M., Janes, M.D., Buell, C.R., Tang, X., Collmer, A., and Alfano, J.R. 2002. Genomewide identification of proteins secreted by the Hrp type III protein secretion system of Pseudomonas syringae pv. tomato DC3000. Proc Natl Acad Sci U S A 99:7652-7657.

Roine, E., Wei, W., Yuan, J., Nurmiaho-Lassila, E., Kalkkinen, N., Romantschuk, M., and He, S. 1997. Hrp pilus: an hrp-dependent bacterial surface appendage produced by Pseudomonas syringae pv. tomato DC3000. Proc Natl Acad Sci USA 94:3459 - 3464.

Schechter, L.M., Vencato, M., Jordan, K.L., Schneider, S.E., Schneider, D.J., and Collmer, A. 2006. Multiple approaches to a complete inventory of Pseudomonas syringae pv. tomato DC3000 type III secretion system effector proteins. Mol Plant Microbe Interact 19:1180-1192.

Shimono, M., Lu, Y.J., Porter, K., Kvitko, B.H., Henty-Ridilla, J., Creason, A., He, S.Y., Chang, J.H., Staiger, C.J., and Day, B. 2016. The Pseudomonas syringae Type III Effector HopG1 Induces Actin Remodeling to Promote Symptom Development and Susceptibility during Infection. Plant Physiol 171:2239-2255.

Singh, R., Lee, S., Ortega, L., Ramu, V.S., Senthil-Kumar, M., Blancaflor, E.B., Rojas, C.M., and Mysore, K.S. 2018. Two Chloroplast-Localized Proteins: AtNHR2A and AtNHR2B, Contribute to Callose Deposition During Nonhost Disease Resistance in Arabidopsis. Molecular Plant-Microbe Interactions 31:1280-1290.

Wei, H.L., Zhang, W., and Collmer, A. 2018. Modular Study of the Type III Effector Repertoire in Pseudomonas syringae pv. tomato DC3000 Reveals a Matrix of Effector Interplay in Pathogenesis. Cell Rep 23:1630-1638.

Wilton, M., and Desveaux, D. 2010. Lessons learned from type III effector transgenic plants. Plant Signal Behav 5:746-748.

Wilton, M., Subramaniam, R., Elmore, J., Felsensteiner, C., Coaker, G., and Desveaux, D. 2010a. The type III effector HopF2Pto targets Arabidopsis RIN4 protein to promote Pseudomonas syringae virulence. Proc Natl Acad Sci U S A 107:2349-2354.

Xin, X.F., and He, S.Y. 2013. Pseudomonas syringae pv. tomato DC3000: A Model Pathogen for Probing Disease Susceptibility and Hormone Signaling in Plants. Pages 473-498 in: Annual Review of Phytopathology, Vol 51, N.K. VanAlfen, ed. Annual Reviews, Palo Alto.

Xin, X.F., Kvitko, B., and He, S.Y. 2018. Pseudomonas syringae: what it takes to be a pathogen. Nature Reviews Microbiology 16:316-328.

Zhang, J., Shao, F., Li, Y., Cui, H., Chen, L., Li, H., Zou, Y., Long, C., Lan, L., Chai, J., Chen, S., Tang, X., and Zhou, J.M. 2007. A Pseudomonas syringae effector inactivates MAPKs to suppress PAMP-induced immunity in plants. Cell host & microbe 1:175-185.

3.6 Figures

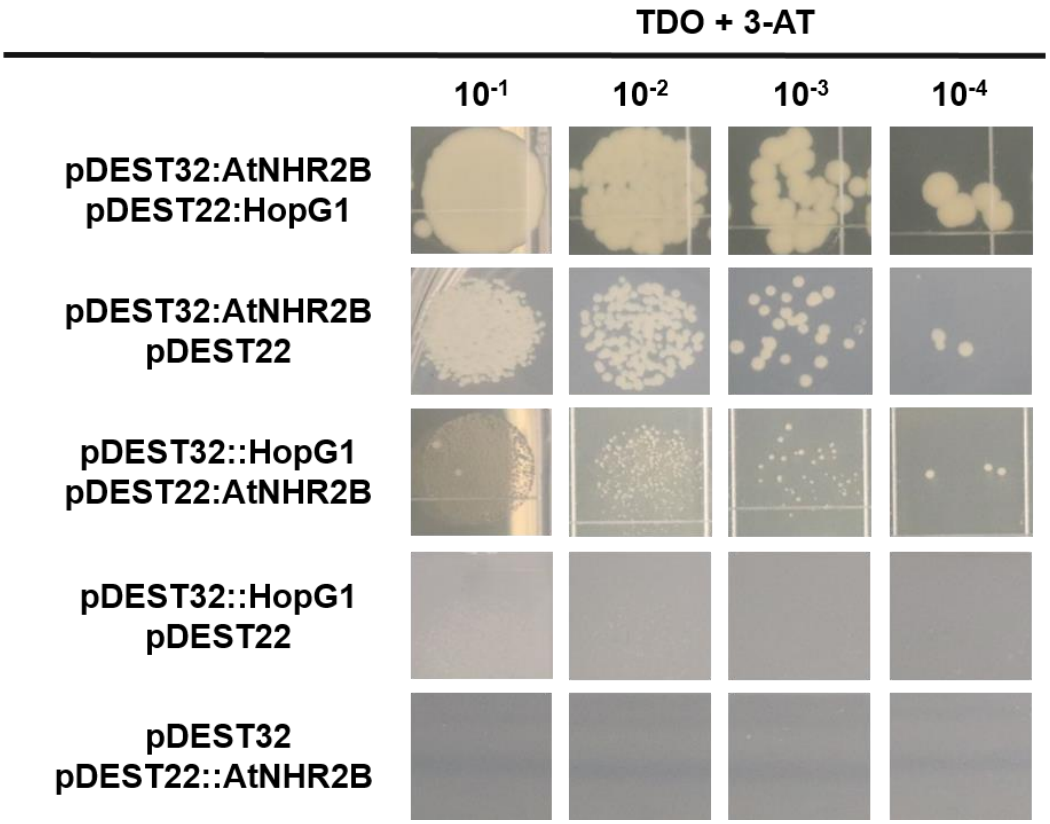

Figure 1. AtNHR2B interacts with HopG1 in yeast. Yeast strain MaV203 was transformed with bait (*pDEST32*) and prey (*pDEST22*) in the following combinations: *pDEST32*::*AtNHR2B* + *pDEST22*::*HopG1*; *pDEST32*::*AtNHR2B* + *pDEST22*; *pDEST22*::*AtNHR2B* + *pDEST32*::*HopG1*; *pDEST32*::*HopG1* + *pDEST22* and *pDEST32* + *pDEST22*::*AtNHR2B*. Transformants were initially recovered in double drop out (DDO) media, transfer to liquid DDO, serially diluted in plated on triple drop out media (TDO) (-leu, -trp, -his) supplemented with 15mM 3-AT, to evaluate yeast growth.

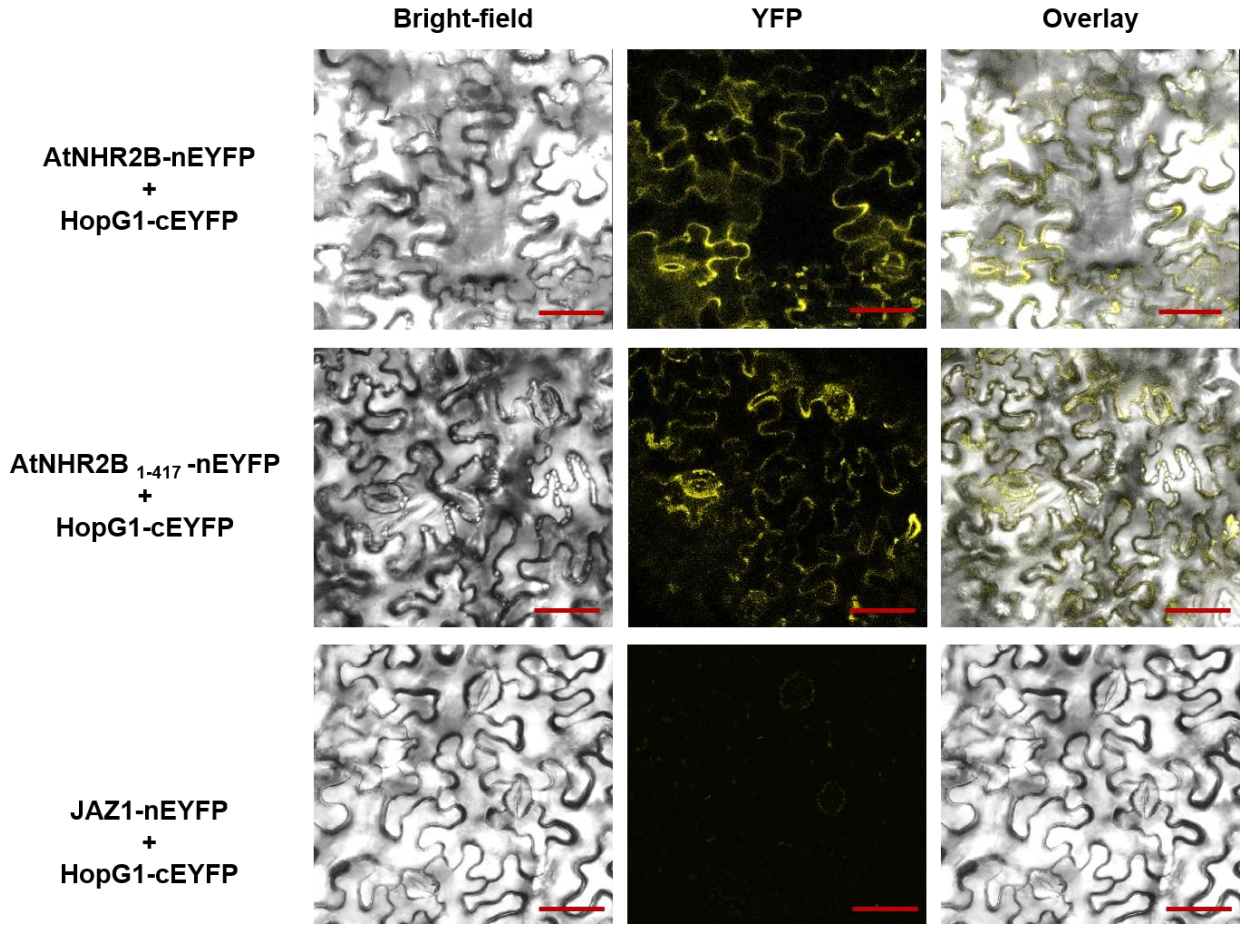

Figure 2. AtNHR2B interacts with the Pst DC3000 effector HopG1 in planta. *AtNHR2B*, the truncated version of *AtNHR2B* (*AtNHR2B*$_{1-417}$) and *JAZ1* were fused to the N-terminal fragment of EYFP to generate *AtNHR2B-nEYFP*, *AtNHR2B*$_{1-417}$*-nEYFP* and *JAZ1-nEYFP*. *HopG1* was fused to the C-terminal fragment of EYFP to generate *HopG1-cEYFP*. N-terminal EYFP fusions were individually co-infiltrated with HopG1-cEYFP fusion into *N. benthamiana* plants. After 48 hpi, infiltrated plants were imaged by laser scanning confocal microscopy using excitation of 514 nm and emission 500-530 nm. Scale bar = 50 µm. Images were taken in bright and fluorescent fields and both fields are shown in the overlay

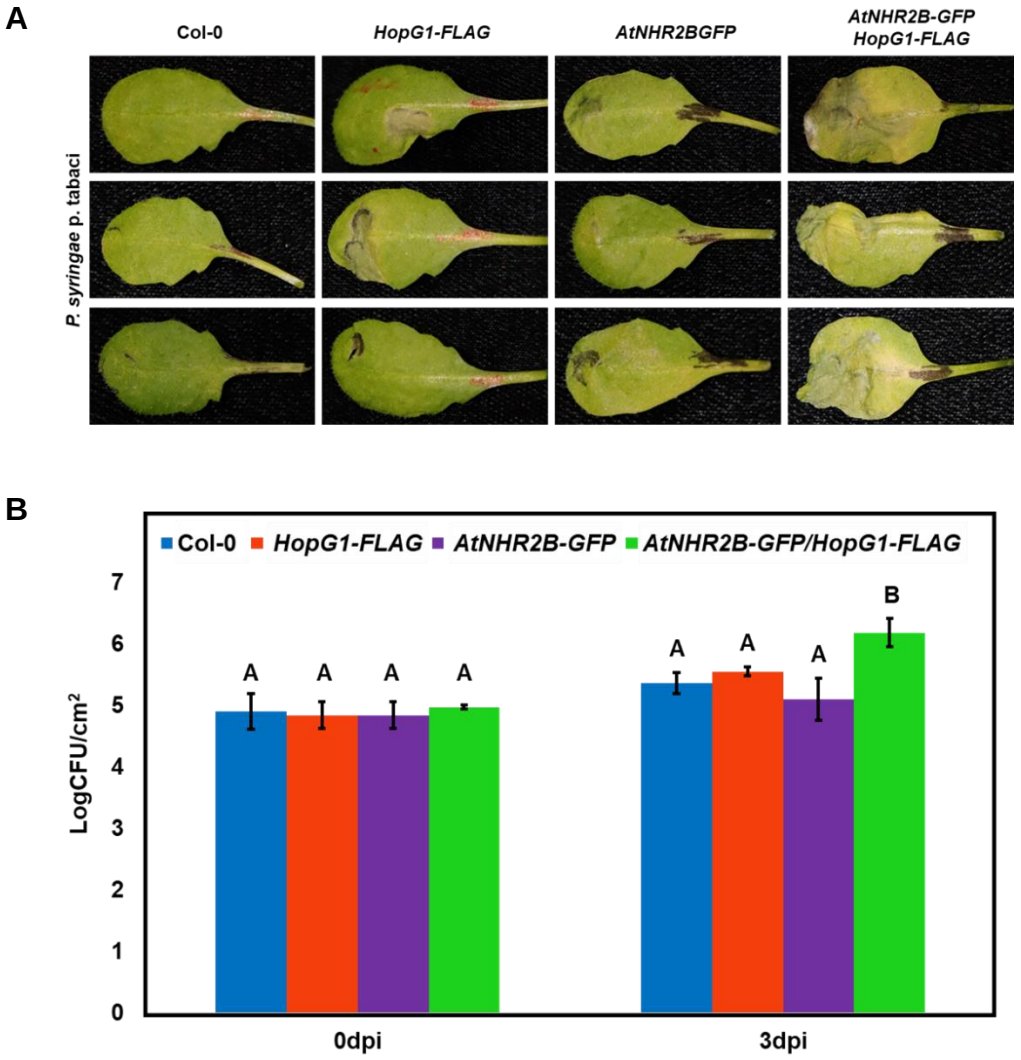

Figure 3. *Arabidopsis* plants expressing *HopG1-FLAG* inoculated with the non-adapted pathogen *P. syringae* pv. tabaci exhibit AtNHR2B-dependent phenotypes. Wild-type Col-0 and transgenic plants expressing *HopG1-FLAG*, *AtNHR2B-GFP* and *AtNHR2B-GFP/HopD1-FLAG* were syringe-inoculated with the non-adapted bacterial pathogen *P. syringae* pv. tabaci at OD_{600}= 0.02 (1 x 10^7CFU/ml), to evaluate disease symptoms at 5 dpi **(A)** and to quantify bacterial growth at 0 and 3 dpi **(B).** Bars represent the means and standard deviation for three independent experiments. Kruskal-Wallis test was used to test significant differences. Letter represent significant difference with P ≤ 0.05. Same letters above bars indicate not statistically significant difference.

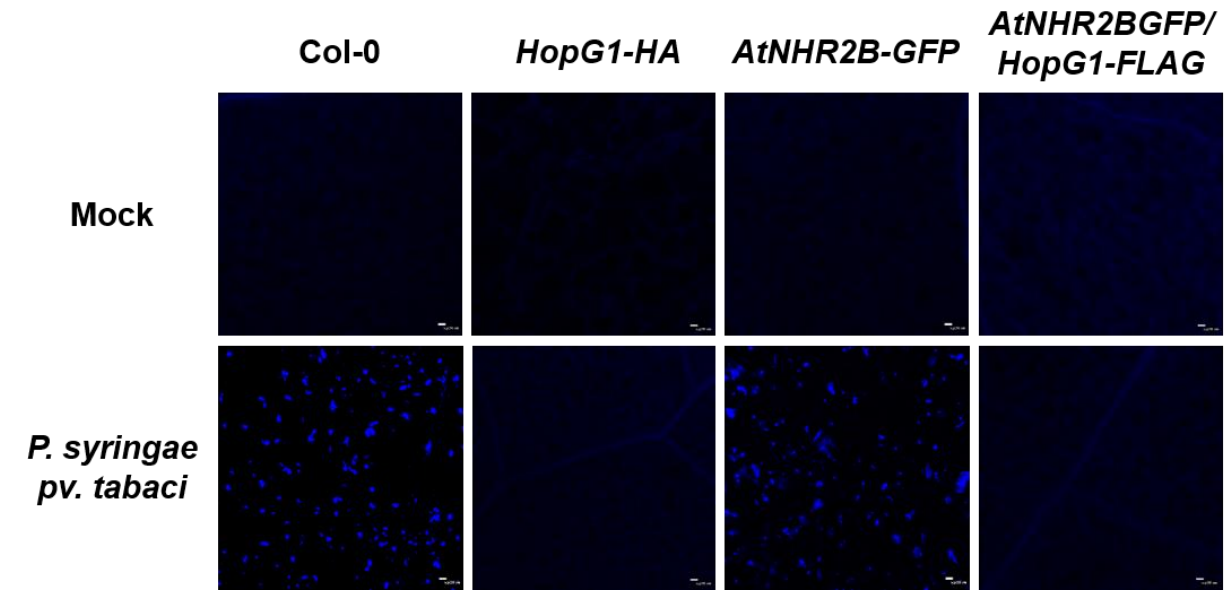

Figure 4. *Arabidopsis* plants expressing the bacterial effector *HopG1-FLAG* are deficient in callose deposition. Wild-type Col-0 and transgenic plants expressing *HopG1-FLAG*, *AtNHR2B-GFP* and *AtNHR2B-GFP/HopD1-FLAG* were syringe-inoculated with the non-adapted bacterial pathogen *P. syringae* pv. tabaci at OD_{600}= 0.02 (1 x 10^7CFU/ml). Inoculated leaves were detached at 24 hpi and stained with 5% aniline blue staining to asses callose deposition. Images were taken using a confocal microscope under DAPI filter. Scale bar = 20 µm.

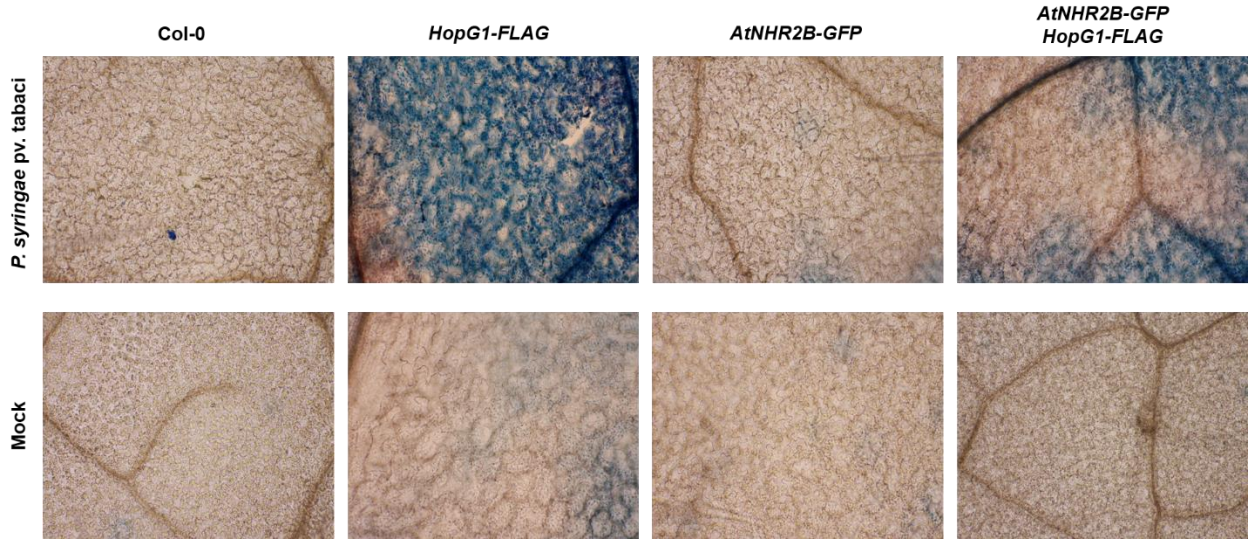

Figure 5. *Arabidopsis* plants over-expressing HopG1-FLAG showed cell death phenotype upon inoculation with the nonadapted pathogen *P. syringae* pv. tabaci. Wild-type Col-0 and transgenic plants expressing *HopG1-FLAG*, *AtNHR2B-GFP* and *AtNHR2B-GFP/HopG1-FLAG* were syringe inoculated with the nonadapted bacterial pathogen *P. syringae* pv. tabaci at OD_{600}= 0.02 (1 x 10^7CFU/ml). Leaves were detached at 24 hpi and stained with 0.05% trypan blue to evaluate cell death. Images were taken under brightfield.

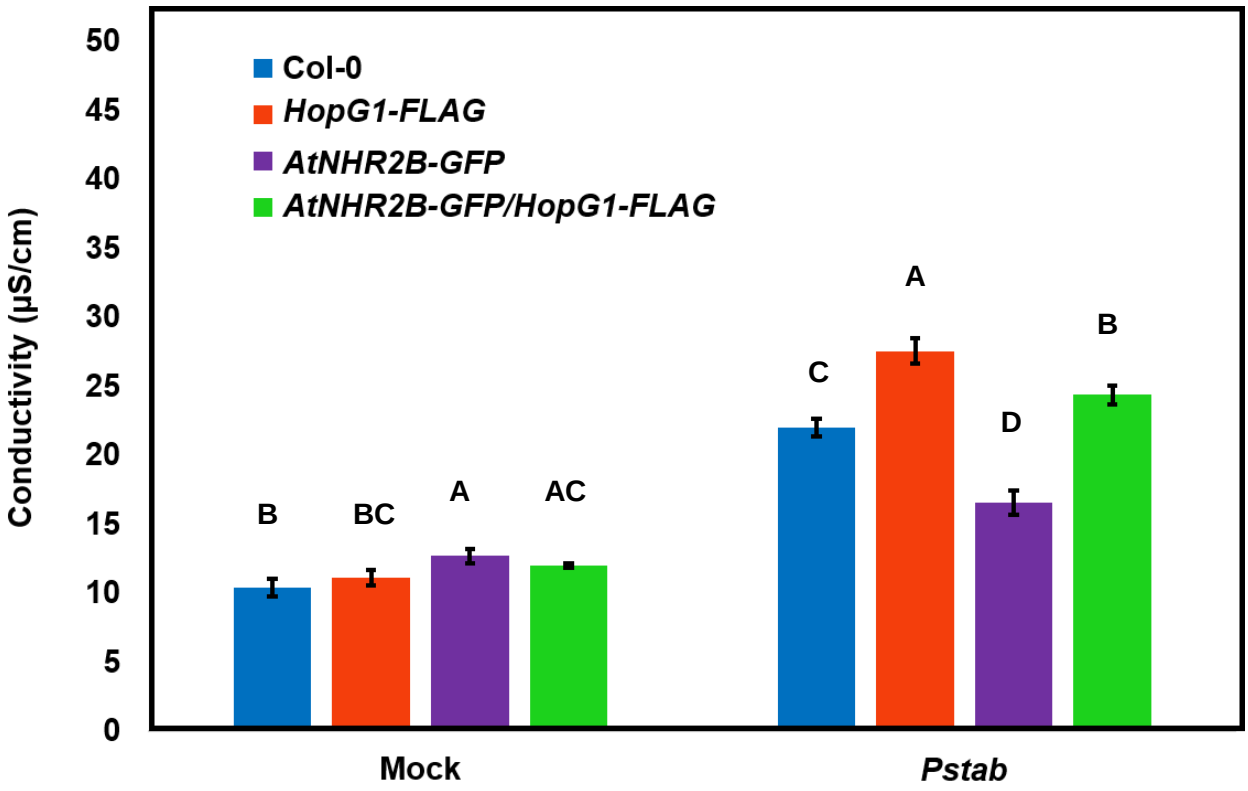

Figure 6. *Arabidopsis* plants over-expressing *HopG1-FLAG* showed high ion leakage levels upon inoculation with the nonadapted pathogen *P. syringae* pv. *tabaci*. Wild-type Col-0 and transgenic plants expressing *HopG1-FLAG*, *AtNHR2B-GFP* and *AtNHR2B-GFP/HopG1-FLAG* were syringe inoculated with the nonadapted bacterial pathogen *P. syringae* pv. tabaci at OD_{600}= (1 x 10^7CFU/ml). At 24 hpi, six leaf disks per genotype were collected to generate three replicates, two leaf disks per replicate. Collected tissue was placed in a 50 mL falcon tube with 15 mL of ddH_2O and agitated at room temperature. Conductivity measured after 3 h. One-way ANOVA was used to test significant differences. Letter represent significant difference with $P \leq 0.05$. Same letters above bars indicate not statistically significant difference.

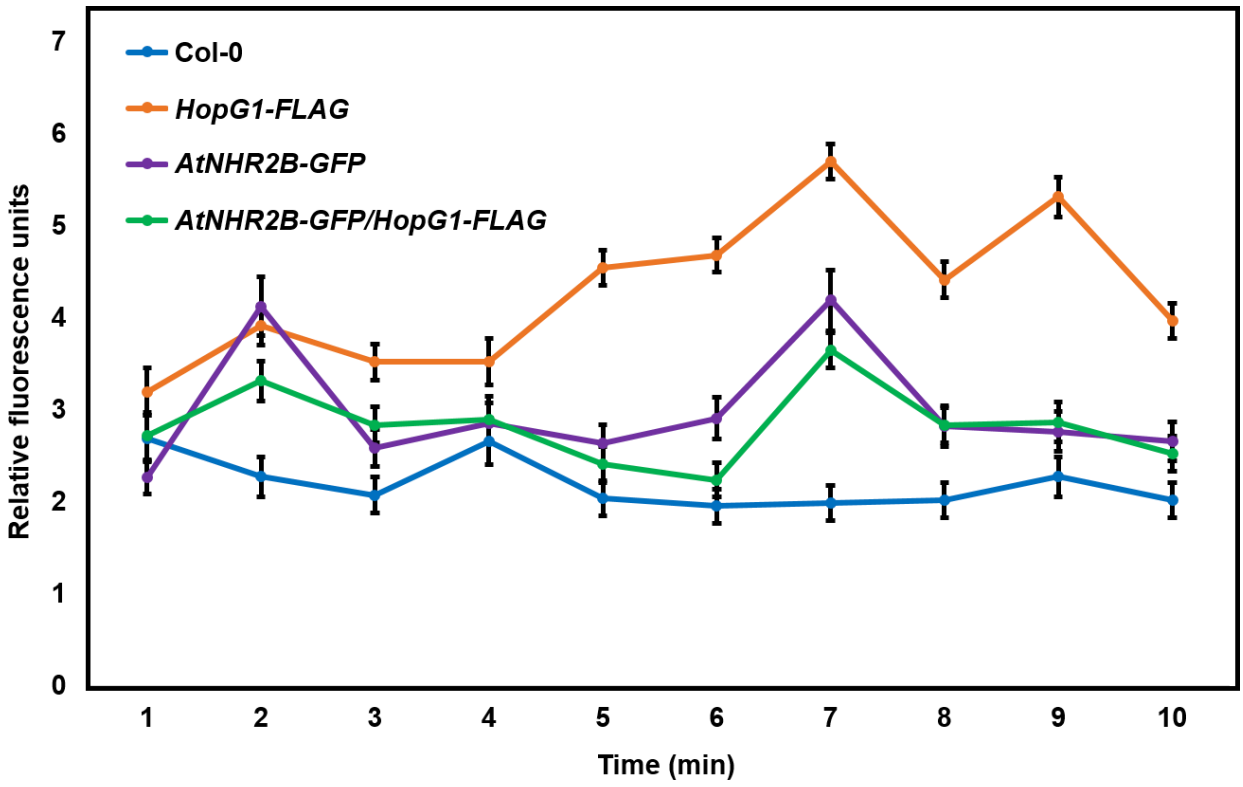

Figure 7. *Arabidopsis* plants over-expressing HopG1-FLAG showed enhanced ROS levels upon inoculation with the non-adapted pathogen *P. syringae* pv. *tabaci*. Wild-type Col-0 and transgenic plants expressing *AtNHR2B-GFP*, *HopG1-FLAG* and *AtNHR2B-GFP*/*HopG1-FLAG* plants were used to collect leaf disks cut out using a 1.2 cm core-borer. Leaf disks from each genotype were transferred to clear bottom plates for fluorometric analysis and submerged in *Pstab* inoculum at a final concentration of 1 X 10^7 CFU/mL or water for mock-treatment. Two hours after inoculation with either *Pstab* mock-treatment, MitoTracker Red CM-H_2XRos (ThermoFisher Scientific) was added at a final concentration of 0.005 mM and incubated for ten minutes before taking the first reading. Fluorescence was measured with an excitation wavelength of 570 nm and an emission wavelength of 535 nm on BioTek luminescence microplate reader in intervals of 10 minutes.

4 HopD1 *a Pseudomonas syringae* pv. tomato DC3000 Effector Targets AtNHR2B, and Interferes with its Role in Plant Immunity

4.1 Introduction

Pseudomonas syringae is a plant pathogenic Gram-negative bacterium, and one of the most important bacterial pathogens as it causes disease in a wide range of plants (Xin et al., 2018). *P. syringae* has been divided into more than 50 pathovars depending on the host specificity. Among those, *Pseudomonas syringae* pv. tomato DC3000 (*Pst* DC3000) that infects tomato and the model plant *Arabidopsis thaliana* has been the source of intense investigations and the paradigm to dissect the molecular and cellular interactions between plants and plant pathogenic bacteria (Xin and He, 2013).

The pathogenicity of *Pst* DC3000 is mostly associated with the type III secretion system (T3SS), a complex of proteins that spans the inner and outer bacterial membranes and delivers inside the plant cytoplasm bacterial proteins known as effectors (Xin and He, 2013). Translocation of *Pst* DC3000 effectors into the plant cytoplasm trigger two different outcomes depending on the infected plant. In non-host plants, type III secreted effectors (T3E) can trigger the hypersensitive response (HR), a defense associated mechanism of programmed cell death (Collmer et al., 2000; Lindeberg et al., 2012). In host plants, effector translocation promotes bacterial parasitism by targeting physiological processes and interfering with the plant immune system (Buttner, 2016; Macho, 2016).

Upon plant infection, *Pst* DC3000 delivers into the plant up to 29 different T3E. These effectors work together to allow bacteria to cause disease and proliferate in the plant tissue (Cunnac et al., 2011). Many effectors act redundantly, with several effectors targeting the same plant proteins, or, individual effectors targeting multiple plant proteins (Deslandes and Rivas, 2012). Thus, the

interactions among effectors and their targets are very complex (Lindeberg et al., 2012; Shames and Finlay, 2012). Effector redundancy makes the study of effector function particularly challenging and, consequently, investigating the function of individual effectors relies on strategies that reduce this complexity. These strategies have included using bacterial poly-mutants, with deletions of multiple effectors, to infer whether these deletions allow plant recognition and/or compromise the ability of bacteria to cause disease. Further analysis of phenotypes had enabled characterization of potential plant targets (Kvitko et al., 2009; Cunnac et al., 2011; Wei et al., 2015). Another approach is the generation of transgenic plants expressing single effectors to evaluate gain-of-function phenotypes (Wilton and Desveaux, 2010).

The goal of this work was to identify T3E interfering with plant defense responses. Work in the Rojas' lab has uncovered an *Arabidopsis thaliana* protein that contributes to nonhost resistance and named AtNHR2B (*Arabidopsis thaliana* nonhost resistance 2B). Nonhost resistance enables plants to withstand the deleterious effects of most pathogens due to the integration of preformed and inducible defenses that allow plants to recognize and kill potential pathogens (Senthil-Kumar and Mysore, 2013). AtNHR2B contributes to nonhost resistance by participating in the deposition of the β,-1-3 glucan polymer callose to the cell wall (Singh et al., 2018). Presumably, the deposition of callose to the cell wall provides additional strength to reduce tissue damage (Luna et al., 2011).

This work initially used *Pst* DC3000 poly-mutant strains to narrow down potential effectors interacting with AtNHR2B. This approach revealed HopD1. HopD1 was previously identified as a suppressor of the hypersensitive response (HR), a plant defense response characterized by cell death and triggered by the intracellular recognition of pathogen also known as effector trigger immune (ETI) (Block et al., 2014). Interestingly, HopD1 did not suppress PAMP-triggered immunity (PTI), another branch of plant immunity that recognizes common features in

microbes/pathogens known as MAMPs/ PAMPs (Microbe/Pathogen-Associated Molecular Patterns) (Block et al., 2014). This work showed that HopD1 interacts with AtNHR2B, and transgenic expression of *HopD1* compromises callose deposition and enabling the non-adapted pathogen *P. syringae* pv. tabaci (*Pstab*) to cause disease and grow. Suppression of defense responses mediated by HopD1 was related to the downregulation of PMR4 (Powdery Mildew Resistance 4) that encodes callose synthase.

4.2 Material and methods

4.2.1 Bacterial Strains

P. syringae and *A. tumefaciens* strains used in this study are listed in Table 1.

P. syringae strains were grown at 30° C in King's B (KB) medium supplemented with rifampicin at a final concentration of 25 µg/mL. *A. tumefaciens* strains were grown at 28°C in Luria-Bertani (LB) medium supplemented with kanamycin (25 µg/mL) and rifampicin (50 µg/mL).

4.2.2 Plant Materials and Growth Conditions

A. thaliana seeds were planted in soil and grown for 6 weeks under growth chamber conditions at 21 °C with a 10/14 h light/dark cycle.

N. benthamiana plants were planted in soil and grown for 4 weeks under growth chamber conditions at 25° C with a 10/14 h light/dark cycle.

4.2.3 Plant Inoculation

Five-week-old wild-type Col-0 and *Atnhr2b* mutant plants grown on soil, were syringe-inoculated with wild-type *Pst* DC3000 and the bacterial mutants CUCPB5440, CUCPB5452, CUCPB5500, CUCPB5515, CUCPB5516 at 1 X 10^7 CFU/mL. At 0 and 3 dpi, leaf disks were collected with a 0.5 cm^2 core-borer, ground in 100 µl ddH_2O, serially diluted and plated on KB agar. Each genotype

had four replications and the experiment was repeated three times. Symptoms were evaluated from at 3 and 6 dpi.

To evaluate disease symptoms, bacterial growth and callose deposition in transgenic plants expressing *HopD1*, five-week-old wild-type Col-0, *AtNHR2B-GFP*, *HopD1-HA* and *AtNHR2B-GFP/HopD1-HA* plants grown on soil were syringe-inoculated with *Pstab* at 1 X 10^7 CFU/mL. At 0 and 3 dpi, leaf disks were collected with a 0.5 cm^2 core-borer, ground in 100 µl ddH_2O, serially diluted and plated on KB agar. Each genotype had four replications and the experiment was repeated three times. Symptoms were evaluated from at 3 and 6 dpi.

To evaluate gene expression, six-week-old wild type Col-0, *AtNHR2B-GFP*, *HopD1-HA* and *AtNHR2B-GFP*/*HopD1-HA* plants grown *in vitro* in Murashige and Skoog (MS) media, were flood-inoculated with *Pstab* at 1 X 10^7 CFU/mL supplemented with 0.01% silwet, as previously described (Ishiga et al., 2011).

4.2.4 Co-immunoprecipitation

A. tumefaciens harboring *AtNHR2B-GFP*, *HopD1-HA* and free *GFP* were cultured overnight. Overnight cultures were collected, resuspended in induction buffer (20mM MES pH 5.5; 3% sucrose, 200µM acetosyringone) and incubated with constant agitation at room temperature for four hours. Induced cultures were adjusted to a final concentration of OD_{600}=0.3. *A. tumefaciens* harboring *HopD1-HA* was co-infiltrated either with *A. tumefaciens* strains harboring *AtNHR2B-GFP* or *A. tumefaciens* harboring free *GFP.*

Infiltrated leaves were collected at 3 days post-infiltration and tissue was ground in liquid nitrogen for protein extraction. Tissue powder was homogenized in 5 mL of co-immunoprecipitation extraction buffer (100 mM Tris-HCl, pH 7.5, 150 mM NaCl, 1 mM EDTA, 10 mM MgCl2, 10% Glycerol, 0.2% Nonidet P-40, 1 mM PMSF, 5 mM DTT, 1X Proteinase inhibitor cocktail (Sigma

Aldrich, St. Louis, MO). Upon buffer treatment protein extracts were incubated for 30 min on ice and centrifuged at 4°C for 30 min at 13,000 rpm. Supernatants containing extracted proteins were collected in a pre-chilled 50 mL falcon tube.

Protein concentration was measured by Bradford Assay (BioRad, Hercules, CA) and protein expression was confirmed by running protein samples into a SDS-PAGE gel followed by Western blot with Anti-GFP-HRP (1:1000 dilution; Miltenyi Biotec, Auburn, CA) and Anti-HA-HRP (1:1000 dilution; Thermo Fisher Scientific Inc, Carlsbad, CA) and detected by luminol solution (ImmunoCruz, SantaCruz Biotechnology Inc, Dallas, TX).

One milligram of total protein extract was mixed with 20 µl of PierceTM HA Epitope Tag Antibody conjugated to agarose beads (ThermoFisher Scientific) and incubated overnight at 4°C with end to end rocking. After incubation, protein complexes bound to beads were washed three times with 1X TBS buffer (50 mM Tris-HCl, 150 mM NaCl, pH 7.5). Protein complexes bound to the beads were eluted in 2x SDS protein loading buffer, loaded and ran into an SDS-PAGE gel and transferred to nitrocellulose membranes. Proteins were detected by Western Blot by incubating the nitrocellulose membrane with anti-GFP-HRP (1:1000 dilution; Miltenyi Biotec, Auburn, CA) antibodies to detect AtNHR2B-GFP or free GFP or anti-HA-HRP (1:1000 dilution; Thermo Fisher Scientific Inc, Carlsbad, CA) antibodies to detect HopG1-HA, and detected by luminol solution (ImmunoCruz, SantaCruz Biotechnology Inc, Dallas, TX).

4.2.5 Co-localization Experiments

A. tumefaciens containing either *AtNHR2B-RFP* and *HopD1-GFP* were induced, adjusted to an OD_{600} = 0.3 and co-infiltrated into 4-week-old *N. benthamiana* plants for transient expression. Inoculated leaves were collected 3 dpi and images were taken by the laser confocal microscope Leica SP5, using the RFP channel with an excitation wavelength of 570 nm and an emission

wavelength of 657 nm, and the GFP channel with an excitation wavelength of 496 nm and an emission wavelength of 549 nm.

4.2.6 Callose Deposition

Six to nine leaves from six independent plants for each genotype and inoculated with *Pstab* or infiltrated with water were detached after 24 hpi and stained with 5% aniline blue to visualize callose deposits (Kvitko et al., 2009a). Images were taken by Nikon 90i upright scanning laser confocal microscope (Nikon) using a DAPI (4',6-diamidino-2-phenylindole) filter with excitation wavelength of 405 nm and an emission wavelength of 450-510 nm.

4.2.7 RNA Extraction and cDNA Synthesis

Twelve plants inoculated with *Pstab* and mock-treated plants from each genotype were harvested by collecting rosettes in liquid nitrogen 12 hpi. Samples were further ground for RNA extraction using the TRIzol reagent followed by DNAse treatment using TURBO DNA-free kit (Thermo Fisher Scientific). Purified RNA was used for cDNA synthesis using the High Capacity cDNA Reverse Transcription kit (Thermo Fisher Scientific).

4.3 Results

4.3.1 Use of *Pst* DC3000 Mutants to Narrow Down Potential Effectors Targeting *AtNHR2B*

In order to identify T3SE targeting AtNHR2B, five *Pst* DC300 poly-mutants lacking combinations of effectors (Kvitko et al., 2009) were used (Table 1). Collectively, these mutants represent the deletion of 18 effectors. Those poly-mutants have a significant reduction in virulence in comparison when the wild-type strain *Pst* DC3000, when inoculated in wild-type tomato, *N. benthamiana* and *Arabidopsis* plants (Kvitko et al., 2009; Shimono et al., 2016). Thus, the rationale of this study is that inoculating these mutants in plants deficient in defense responses

would enable them to cause disease when their respective plant targets are absent. Using that rationale, wild-type *Pst* DC3000 and the poly-mutant strains were inoculated in wild-type Col-0 as well as in the *Atnhr2b* mutant. Inoculation of wild-type *Ps t*DC3000 caused localized chlorosis in wild-type Col-0 plants as previously reported (Shimono et al., 2016), but more extensive chlorosis was observed on the *Atnhr2b* mutant plants (Figure 1A). In spite of the differences in symptoms caused by *Pst* DC3000 in wild-type Col-0 and the *Atnhr2b* mutant, there was no difference in bacterial growth at 3dpi (Figure 1B).

The mutant strains CUCPB5440, CUCPB5452, CUCPB5515 were unable to cause disease in Col-0, but caused different symptoms in the *Atnhr2b* mutant. CUCPB5440 caused severe chlorosis and wilting of the leaves, while CUCPB5452 and CUCPB5515 caused mild discoloration. CUCPB5500 showed reduced virulence in wild-type Col-0 but enhanced virulence on the *Atnhr2b* mutant. CUCPB5516 showed reduced virulence in both Col-0 and the *Atnhr2b* mutant.

CUCPB5440 showed 1 log reduction in growth at 3 dpi in comparison with wild-type *Pst*DC3000, and that reduction in growth was observed in both wild-type Col-0 and the *Atnhr2b* mutant. The other mutants CUCPB5452, CUCPB5500, CUCPB5515 and CUCPB5516 showed ~1.5 log reduction in growth at 3 dpi in comparison with wild-type *Pst*DC3000 and that reduction in growth was similar in wild-type Col-0 and the *Atnhr2b* mutant.

Altogether these results suggest that the absence of these effectors reduce the ability of *Pst* DC3000 to grow in plants without eliminating it and that the absence of functional AtNHR2B do not enhance bacterial growth. However, the data shows that particular combinations of effectors are required to successfully produce disease symptoms and, in that scenario the absence of *AtNHR2B* contributes to the disease outcome. Because CUCBP5440, CUCPB5452 and

CUPB5515 had the most striking phenotypes of not causing disease in wild-type Col-0 but causing disease in the *Atnhr2b* mutant, this phenotype might be due a common effector or set of effectors among those strains. CUCPB5440, CUPCB5452 and CUCPB5515 lack cluster IV that includes effectors HopD1 and HopR1. The possible targeting of AtNHR2B by HopD1 was further investigated.

4.3.2 HopD1 Interacts and Co-localizes with AtNHR2B-GFP *in Planta*

As a first approach to evaluate that HopD1 targets AtNHR2B, it is necessary to investigate their physical interaction, and that interaction was examined *in planta* by transient expression in *N. benthamiana* followed by co-immunoprecipitation. Immunoprecipitation of HopD1-HA with anti-HA antibodies co-immunoprecipitated AtNHR2B-GFP but not free GFP as detected by Western Blot using Anti-GFP antibodies (Figure 2). These co-immunoprecipitation results showed that HopD1 physically interacts with AtNHR2B and not with the GFP tag.

The interaction detected by co-immunoprecipitation between HopD1-HA and AtNHR2B-GFP led to the hypothesis that both proteins co-localize in planta. Transient co-expression of *HopD1-GFP* and *AtNHR2B-RFP* in *N. benthamiana* followed by visualization using laser scanning confocal microscopy revealed that HopD1-GFP co-localizes with AtNHR2B-RFP, which can be seen as the overlapping signal of both proteins that results in the emission of a yellow color when both GFP and RFP signals are merged (Figure 3). Moreover, that localization occurs in the cytoplasm, one of the possible localizations of AtNHR2B-GFP (Singh et al., 2018).

4.3.3 Expression of *HopD1 in Planta* Hinders Defense Responses

In order to dissect how HopD1 contributes to the pathogenicity of *Pst DC3000*, transgenic plants expressing *HopD1-HA* were obtained from Dr. Jim Alfano (U. Nebraska, Lincoln) and crossed

with *Arabidopsis* plants expressing *AtNHR2B-GFP.* These plants were inoculated with the with the non-adapted pathogen *Pstab*, that does not cause disease in wild-type Col-0 plants.

As a nonadapted pathogen of *Arabidopsis*, *Pstab* did not cause disease symptoms in wild-type Col-0 plants (Figure 4A) and the numbers of bacteria remain relatively the same between 0 and 3 dpi. Transgenic *Arabidopsis* lines over-expressing *AtNHR2B-GFP* inoculated with *Pstab* did not develop disease symptoms, as expected, because AtNHR2B contributes to disease resistance (Figure 4A). As expected, the numbers of bacteria were reduced after 3 dpi (Figure 4B). However, transgenic plants expressing *HopD1-HA* alone showed disease symptoms characterized by chlorotic lesions that extended beyond the inoculation site, indicating that expression of *HopD1* enables *Pstab* to cause disease symptoms. Interestingly, transgenic plants co-expressing *HopD1-HA* and *AtNHR2B-GFP* showed a reduction in symptoms in comparison with transgenic lines expressing *HopD1-HA alone*, suggesting that overexpression of *AtNHR2B-GFP* alleviate the effects of HopD1. Surprisingly, bacterial growth was comparable between transgenic plants expressing *HopD1-HA* alone and those co-expressing *HopD1-HA* and *AtNHR2B-GFP* (Figure 3B) suggesting that expression of *AtNHR2B-GFP* is sufficient to control the development of symptoms but not enough to control bacterial growth (Figure 4B).

4.3.4 HopD1 Suppresses Callose Deposition

Because AtNHR2B is involved in callose deposition (Singh et al., 2018), it is possible that HopD1 interferes with callose deposition. To test this hypothesis wild-type Col-0, and the transgenic lines *AtNHR2B-GFP*, *HopD1-HA* and *AtNHR2B-GFP/HopD1-HA* were inoculated with the non-adapted pathogen *Pstab*, or mock-treated with water, and inoculated leaves were stained with aniline blue to evaluate callose deposits. Wild-type Col-0 exhibited abundant callose deposits in response to bacterial inoculation and similar levels of callose deposits were observed in transgenic plants overexpressing *AtNHR2B-GFP* (Figure 5). In contrast, *Arabidopsis* plants expressing the bacterial effector *HopD1-HA* alone or in combination with *AtNHR2B-GFP* were completely devoid of callose

deposits (Figure 5), demonstrating that HopD1 interferes with callose deposition and it is able to do so even when *AtNHR2B-GFP* is overexpressed.

4.3.5 HopD1 Downregulates the Expression of Callose Synthase

Callose deposition experiments revealed that transgenic plants expressing *HopD1-HA* and *AtNHR2B-GFP/HopD1-HA* were deficient in depositing callose upon inoculation with the non-adapted pathogen *Pstab*. To evaluate how HopD1 interferes with callose deposition, the expression of the gene *PMR4* (*Powdery Mildew Resistant 4*), that encodes callose synthase, was evaluated by qRT-PCR in wild-type Col-0 and transgenic plants *AtNHR2B-GFP*, *HopD1-HA* and *AtNHR2B-GFP/HopD1-HA.* After inoculation with the non-adapted pathogen *Pstab*, *PMR4* was not expressed in mock-treated plants as previously reported (Ellinger et al., 2014). Inoculation with *Pstab* resulted in *PMR4* induction at 12 hpi in wild-type Col-0 plants (Figure 6). However, lower levels of *PMR4* expression were observed in transgenic plants in comparison with wild-type Col-0. *AtNHR2B-GFP* transgenic plants showed a 2-fold reduction in *PMR4* expression, while *HopD1-HA* and *AtNHR2B-GFP/HopD1-HA* showed ~ 2.5-fold reduction in *PMR4* expression (Figure 6). Similarly, the expression of *PMR4* in *HopD1-HA* and *AtNHR2B-GFP/HopD1-HA* plants was even lower compared to plants of the same genotype that were mock inoculated (Figure 6). These results suggest that plants expressing *HopD1-HA* alone or in combination with *AtNHR2B-GFP/HopG1-HA,* are downregulated in *PMR4* expression although there might be multiple factors contributing to that downregulation as plants overexpressing *AtNHR2B-GFP* are also downregulated in *PMR4* expression in comparison with wild-type Col-0 plants.

4.4 Discussion

This work showed that *Pst*DC3000 polymutants lacking clusters of effectors (Kvitko et al., 2009) are invaluable tools to identify effectors targeting particular plant proteins. Three mutants:

CUCBP5440, CUCPB5452 and CUPB5515 that were avirulent on wild-type Col-0 plants regained virulence on the *Atnhr2b* mutant plants suggesting that common effectors missing in those mutants were dispensable when AtNHR2B was absent. In this case, the common effector was HopD1. Using similar approach HopG1 was identified as an effector targeting the plant actin cytoskeleton (Shimono et al., 2016). Also, HopM1 was found to target the plant protein AtMIN7 based on the ability of the *hopM1* bacterial mutant to grow in the *Atmin7* mutant plant (Nomura et al., 2006).

HopD1, was previously reported to interact and co-localize with NTL9 (Block et al., 2014), an *Arabidopsis* transcription factor belonging to the NAC family (Ooka et al., 2003). This family of transcription factors is related not only with developmental processes, but also with the regulation of stress-related responses (Puranik et al., 2012). This work showed that HopD1 also interacts and co-localizes with AtNHR2B highlighting that HopD1 is another promiscuous effector with more than one target (Lewis et al., 2009; Wei et al., 2018). Although AtNHR2B has putative nuclear localization signals that would suggest a function in transcription (Singh and Rojas, 2018), a direct link between NTL9 and AtNHR2B function has not been established, and the interaction between HopD1 and AtNHR2B was not found in the nucleus but in the cytoplasm. AtNHR2B has a cytoplasmic localization and therefore, the co-localization of HopD1 and AtNHR2B to the cytoplasm agrees with previous results (Singh et al., 2018). However, more work is needed to understand what does this localization of HopD1 and AtNHR2B mean.

HopD1 was previously shown to suppress the hypersensitive response (HR) as demonstrated using transgenic *Arabidopsis* plants expressing HopD1 inoculated with *Pst* DC3000 strains carrying *avrRpm1* or *avrRpt2*. The presence of these two avirulence genes trigger an HR in wild-type Col-0 but this response did not occur in *HopD1* transgenic plants (Block et al., 2014). Similarly, infiltration with an HR inducing strain, *P. fluorescens* carrying *AvrRpm1* resulted in ion

leakage, a marker of cell death. However, ion leakage was not observed after infiltration with *P. fluorescens* carrying *AvrRpm1* and (Block et al., 2014). The finding that suppresses the HR implies that this suppression favors bacterial pathogenicity or enhances plant susceptibility. However, the results from this work showed opposite results. The expression of *HopD1* allowed *Pstab* to cause disease. *Pstab* does not cause disease in wild-type Col-0 plants either because it lacks appropriate collection of effectors to establish compatibility or, because its effectors are recognized by the plant. The first scenario is very likely because HopD1 is not found in *Pstab* (Baltrus et al., 2011), suggesting that in *Pst*DC3000, HopD1 is important to establish compatibility, necessary to cause disease. Therefore, transgenic expression of *HopD1* enables *Pstab* to become pathogenic in *Arabidopsis.* Interestingly, the finding that *Pstab* is able to grow in plants expressing *HopD1-HA* when *AtNHR2B*-GFP is overexpressed without causing significant symptoms shows that symptoms development and bacterial growth are independent processes (Korves and Bergelson, 2003; Develey-Riviere and Galiana, 2007) and that symptoms development occur at later stages of pathogenesis after bacteria have reached a population threshold (Cunnac et al., 2011). Perhaps, AtNHR2B functions at later stages controlling the development of symptoms.

The results from this study, also showed that transgenic expression of *HopD1* abolishes callose deposition in response to inoculation with *Pstab.* Previously, wild-type Col-0 plants inoculated with the HR inducer *P. fluorescens* carrying the avirulence gene *AvrRpm1* showed deposition of callose, but callose was also produced upon inoculation with *P. fluorescens* carrying the avirulence gene *AvrRpm1* and *HopD1* (Block et al., 2014). Moreover, *HopD1*- transgenic plants treated with PAMPs had equivalent levels of callose deposits than wild-type Col-0 treated with PAMPs (Block et al., 2014). The authors concluded that *HopD1* does not affect callose deposition. The results from this study clearly show that HopD1 affects callose deposition and that overexpression of *AtNHR2B-GFP* does not counteract that effect. Moreover, gene expression

analyses of *PMR4*, showed that *HopD1* expression significantly reduced *PMR4* expression. It is not clear why plants expressing *AtNHR2B-GFP* showed reduced levels of *PMR4* expression but normal levels of callose deposits. Further research is needed to fully understand how AtNHR2B contributes to callose deposition.

4.5 References

Baltrus, D.A., Nishimura, M.T., Romanchuk, A., Chang, J.H., Mukhtar, M.S., Cherkis, K., Roach, J., Grant, S.R., Jones, C.D., and Dangl, J.L. 2011. Dynamic Evolution of Pathogenicity Revealed by Sequencing and Comparative Genomics of 19 Pseudomonas syringae Isolates. Plos Pathogens 7:22.

Block, A., Toruno, T.Y., Elowsky, C.G., Zhang, C., Steinbrenner, J., Beynon, J., and Alfano, J.R. 2014. The Pseudomonas syringae type III effector HopD1 suppresses effector-triggered immunity, localizes to the endoplasmic reticulum, and targets the Arabidopsis transcription factor NTL9. New Phytol 201:1358-1370.

Buttner, D. 2016. Behind the lines-actions of bacterial type III effector proteins in plant cells. Fems Microbiology Reviews 40:894-937.

Collmer, A., Badel, J.L., Charkowski, A.O., Deng, W.L., Fouts, D.E., Ramos, A.R., Rehm, A.H., Anderson, D.M., Schneewind, O., van Dijk, K., and Alfano, J.R. 2000. Pseudomonas syringae Hrp type III secretion system and effector proteins. Proceedings of the National Academy of Sciences of the United States of America 97:8770-8777.

Cunnac, S., Lindeberg, M., and Collmer, A. 2009. Pseudomonas syringae type III secretion system effectors: repertoires in search of functions. Curr Opin Microbiol 12:53-60.

Cunnac, S., Chakravarthy, S., Kvitko, B.H., Russell, A.B., Martin, G.B., and Collmer, A. 2011. Genetic disassembly and combinatorial reassembly identify a minimal functional repertoire of type III effectors in Pseudomonas syringae. Proc Natl Acad Sci U S A 108:2975-2980.

Deslandes, L., and Rivas, S. 2012. Catch me if you can: bacterial effectors and plant targets. Trends in Plant Science 17:644-655.

Develey-Riviere, M.P., and Galiana, E. 2007. Resistance to pathogens and host developmental stage: a multifaceted relationship within the plant kingdom. New Phytologist 175:405-416.

Ellinger, D., Glockner, A., Koch, J., Naumann, M., Sturtz, V., Schutt, K., Manisseri, C., Somerville, S.C., and Voigt, C.A. 2014. Interaction of the Arabidopsis GTPase RabA4c with Its Effector PMR4 Results in Complete Penetration Resistance to Powdery Mildew. Plant Cell 26:3185-3200.

Ishiga, Y., Ishiga, T., Uppalapati, S.R., and Mysore, K.S. 2011. Arabidopsis seedling flood-inoculation technique: a rapid and reliable assay for studying plant-bacterial interactions. Plant methods 7:32.

Korves, T.M., and Bergelson, J. 2003. A developmental response to pathogen infection in Arabidopsis. Plant Physiology 133:339-347.

Kvitko, B.H., Park, D.H., Velasquez, A.C., Wei, C.F., Russell, A.B., Martin, G.B., Schneider, D.J., and Collmer, A. 2009a. Deletions in the Repertoire of Pseudomonas syringae pv. tomato DC3000 Type III Secretion Effector Genes Reveal Functional Overlap among Effectors. Plos Pathogens 5:16.

Lewis, J.D., Guttman, D.S., and Desveaux, D. 2009. The targeting of plant cellular systems by injected type III effector proteins. Seminars in Cell & Developmental Biology 20:1055-1063.

Lindeberg, M., Cunnac, S., and Collmer, A. 2012. Pseudomonas syringae type III effector repertoires: last words in endless arguments. Trends Microbiol 20:199-208.

Luna, E., Pastor, V., Robert, J., Flors, V., Mauch-Mani, B., and Ton, J. 2011. Callose Deposition: A Multifaceted Plant Defense Response. Molecular Plant-Microbe Interactions 24:183-193.

Macho, A.P. 2016. Subversion of plant cellular functions by bacterial type-III effectors: beyond suppression of immunity. New Phytol 210:51-57.

Nomura, K., Debroy, S., Lee, Y.H., Pumplin, N., Jones, J., and He, S.Y. 2006. A bacterial virulence protein suppresses host innate immunity to cause plant disease. Science 313:220-223.

Ooka, H., Satoh, K., Doi, K., Nagata, T., Otomo, Y., Murakami, K., Matsubara, K., Osato, N., Kawai, J., Carninci, P., Hayashizaki, Y., Suzuki, K., Kojima, K., Takahara, Y., Yamamoto, K., and Kikuchi, S. 2003. Comprehensive analysis of NAC family genes in Oryza sativa and Arabidopsis thaliana. DNA Research 10:239-247.

Puranik, S., Sahu, P.P., Srivastava, P.S., and Prasad, M. 2012. NAC proteins: regulation and role in stress tolerance. Trends in Plant Science 17:369-381.

Senthil-Kumar, M., and Mysore, K.S. 2013. Nonhost Resistance Against Bacterial Pathogens: Retrospectives and Prospects. Pages 407-+ in: Annual Review of Phytopathology, Vol 51, N.K. VanAlfen, ed. Annual Reviews, Palo Alto.

Shames, S.R., and Finlay, B.B. 2012. Bacterial effector interplay: a new way to view effector function. Trends in Microbiology 20:214-219.

Shimono, M., Lu, Y.J., Porter, K., Kvitko, B.H., Henty-Ridilla, J., Creason, A., He, S.Y., Chang, J.H., Staiger, C.J., and Day, B. 2016a. The Pseudomonas syringae Type III Effector HopG1 Induces Actin Remodeling to Promote Symptom Development and Susceptibility during Infection. Plant Physiology 171:2239-2255.

Singh, R., and Rojas, C.M. 2018. Dissecting the functional domains of the Arabidopsis thaliana nonhost resistance 2B (AtNHR2B) protein. Plant Signal Behav:1-6.

Singh, R., Lee, S., Ortega, L., Ramu, V.S., Senthil-Kumar, M., Blancaflor, E.B., Rojas, C.M., and Mysore, K.S. 2018. Two Chloroplast-Localized Proteins: AtNHR2A and AtNHR2B, Contribute to Callose Deposition During Nonhost Disease Resistance in Arabidopsis. Molecular Plant-Microbe Interactions 31:1280-1290.

Wei, H.L., Zhang, W., and Collmer, A. 2018. Modular Study of the Type III Effector Repertoire in Pseudomonas syringae pv. tomato DC3000 Reveals a Matrix of Effector Interplay in Pathogenesis. Cell Reports 23:1630-1638.

Wei, H.L., Chakravarthy, S., Mathieu, J., Helmann, T.C., Stodghill, P., Swingle, B., Martin, G.B., and Collmer, A. 2015. Pseudomonas syringae pv. tomato DC3000 Type III Secretion Effector Polymutants Reveal an Interplay between HopAD1 and AvrPtoB. Cell Host & Microbe 17:752-762.

Wilton, M., and Desveaux, D. 2010. Lessons learned from type III effector transgenic plants. Plant Signal Behav 5:746-748.

Xin, X.F., and He, S.Y. 2013. Pseudomonas syringae pv. tomato DC3000: A Model Pathogen for Probing Disease Susceptibility and Hormone Signaling in Plants. Pages 473-498 in: Annual Review of Phytopathology, Vol 51, N.K. VanAlfen, ed. Annual Reviews, Palo Alto.

Xin, X.F., Kvitko, B., and He, S.Y. 2018. Pseudomonas syringae: what it takes to be a pathogen. Nature Reviews Microbiology 16:316-328.

4.6 Tables

Table 1. Strains used in this study

Strain	Genotype	Clusters deleted	Resistance
CUCPB5440	ΔhopD1-hopR1::FRT	ΔIV	Rif
CUCPB5452	ΔhopC1-hopH1::FRT ΔhopD1-hopR1b::FRT; ΔhopAA1-2-hopG1::FRT pDC3000A^{--}B^{--}	ΔIIΔIVΔIXΔX	Rif
CUCPB5500	ΔhopU1-hopF2 ΔhopC1-hopH1::FRT ΔhopD1-hopR1::FRT ΔavrE-shcN; ΔhopAA1-2-hopG1::FRT pDC3000A^{--}B^{--}	ΔIΔIIΔIVΔCELΔIXΔX	Rif
CUCPB5515	ΔhopD1-hopR1::FRT ΔavrE-shcN	ΔIVΔCEL	Rif
CUCPB5516	ΔhopD1-hopR1::FRT ΔavrE-shcN pDC3000A-B-	ΔIVΔCELΔX	Rif
P. syringae pv tomato DC3000	WT		Rif
P. syringae pv. tabaci	WT		Rif
Agrobacterium tumefaciens GV3101	pEarlyGate201::HopD1		Kan, rif
Agrobacterium tumefaciens GV3101	pK7WGR2::AtNHR2B		Rif, spec
Agrobacterium tumefaciens GV3101	pK7RWG2::AtNHR2B		Rif, spec
Agrobacterium tumefaciens GV3101	HopD1-GFP		Spec

4.7 Figures

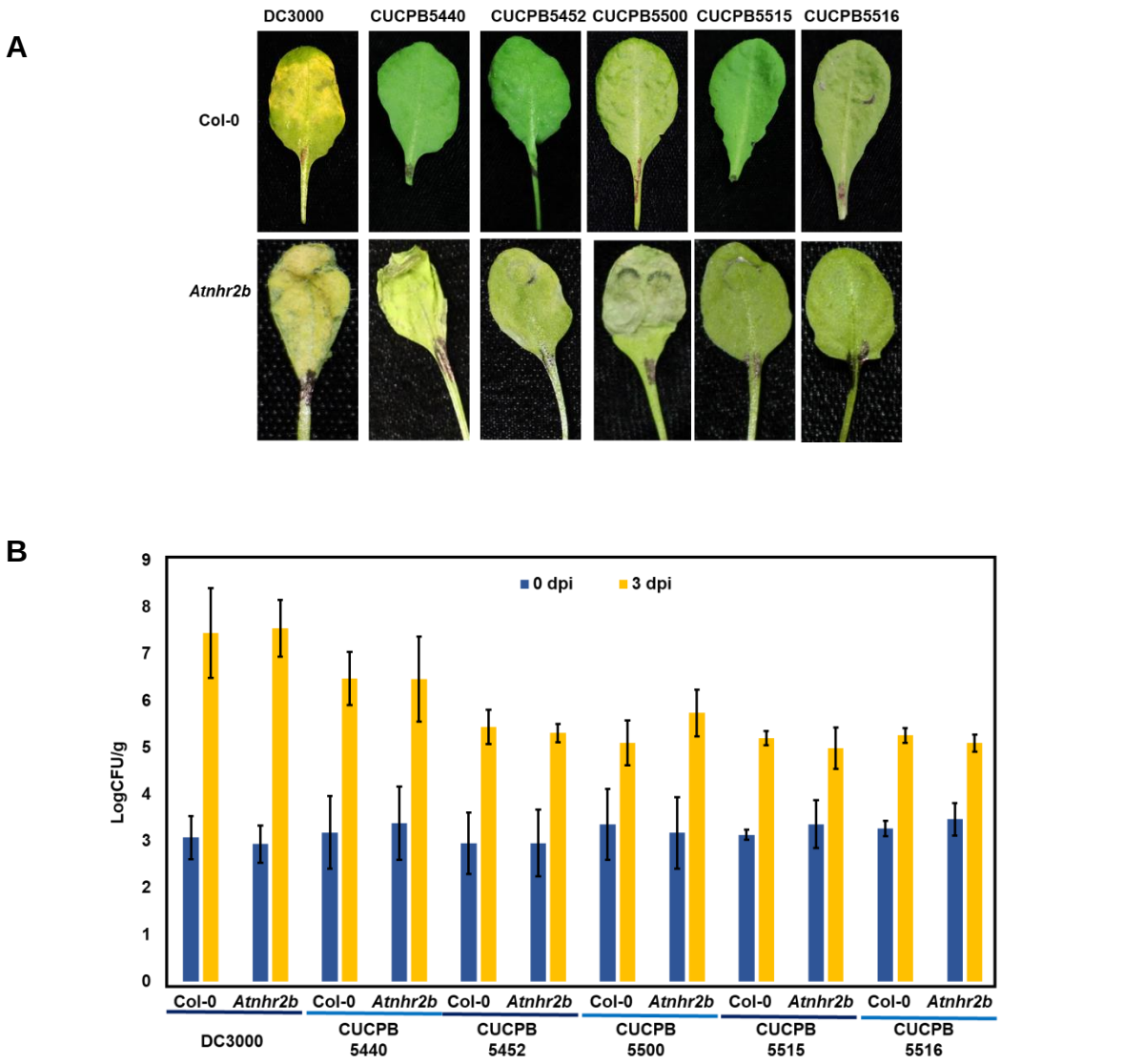

Figure 1. Some *Pseudomonas syringae* pv. tomato DC3000 mutant strains can regain virulence in *Atnhr2b* mutant plants. Wild-type Col-0 and *Atnhr2b* mutant plants were syringe-inoculated with the adapted bacterial pathogen *P*st DC3000 and the bacterial mutants CUCPB5440, CUCPB5452, CUCPB5500, CUCPB5515, CUCPB5516 at OD_{600}= 0.02 (1x 10^7CFU/ml) to evaluate disease symptoms at 5 dpi **(A)** and to quantify bacterial populations at 0 and 3 dpi **(B)**. Bars represent means and standard deviation for three replications.

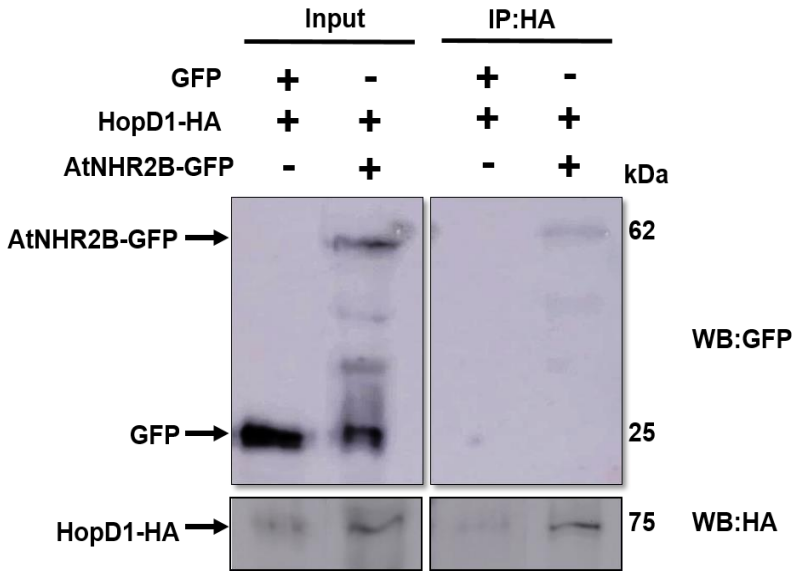

Figure 2. HopD1 interacts AtNHR2B *in planta*. *Agrobacterium tumefaciens* strains harboring *HopD1-HA* and *AtNHR2B-GFP* were co-infiltrated into four-weeks *N. benthamiana* plants for transient expression. As control *Agrobacterium tumefaciens* harboring *HopD1-HA* was co-infiltrated with *Agrobacterium tumefaciens* harboring a construct expressing *35S-GFP*. Infiltrated leaves were harvested for protein extraction followed by immunoprecipitation using anti-HA antibodies. Immunoprecipitated samples were separated by SDS-PAGE electrophoresis and transferred to a nitrocellulose membrane for Western Blot analysis using anti-HA and anti-GFP antibodies.

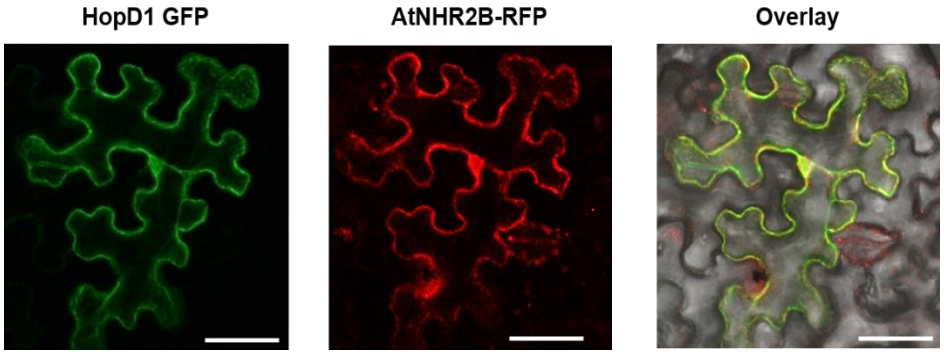

Figure 3. AtNHR2B co-localizes with HopD1. *Agrobacterium tumefaciens* strains harboring *AtNHR2B-RFP* and *HopD1-GFP* were co-infiltrated into four-weeks *N. benthamiana* plants for transient expression. A laser scanning confocal microscope was used to detect the fluorescence at 48 hpi. Green fluorescence was visualized using the GFP channel with an excitation wavelength of 496 nm and an emission wavelength of 549 nm. Red fluorescence was visualized using the RFP channel with an excitation wavelength of 570 nm and an emission wavelength of 657 nm. Scale bar = 50 µm

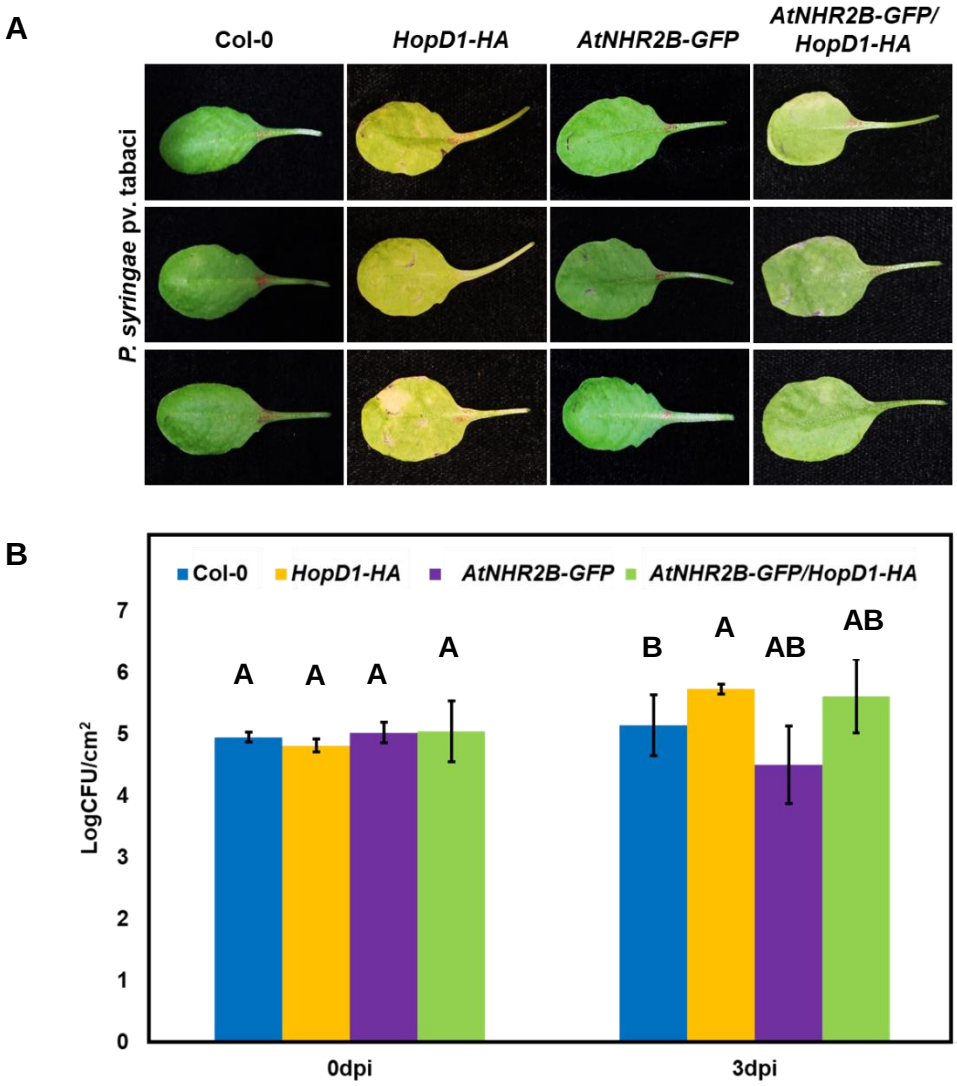

Figure 3. *Arabidopsis* plants expressing the bacterial effector *HopD1* are more susceptible to the non-adapted pathogen *P. syringae* pv. tabaci. Wild-type Col-0 and transgenic plants expressing *HopD1-HA*, *AtNHR2B-GFP* and *AtNHR2B-GFP/HopD1-HA* were syringe-inoculated with the non-adapted bacterial pathogen *P. syringae* pv. tabaci at OD_{600}= 0.02 (1 x 10^7CFU/ml) to evaluate disease symptoms at 5 dpi **(A)** and to quantify bacterial populations at 0 and 3 dpi **(B).** A Kruskal-Wallis test was used to test significant differences. Letter represent significant difference with P ≤ 0.05. Same letters above bars indicate not statistically significant difference.

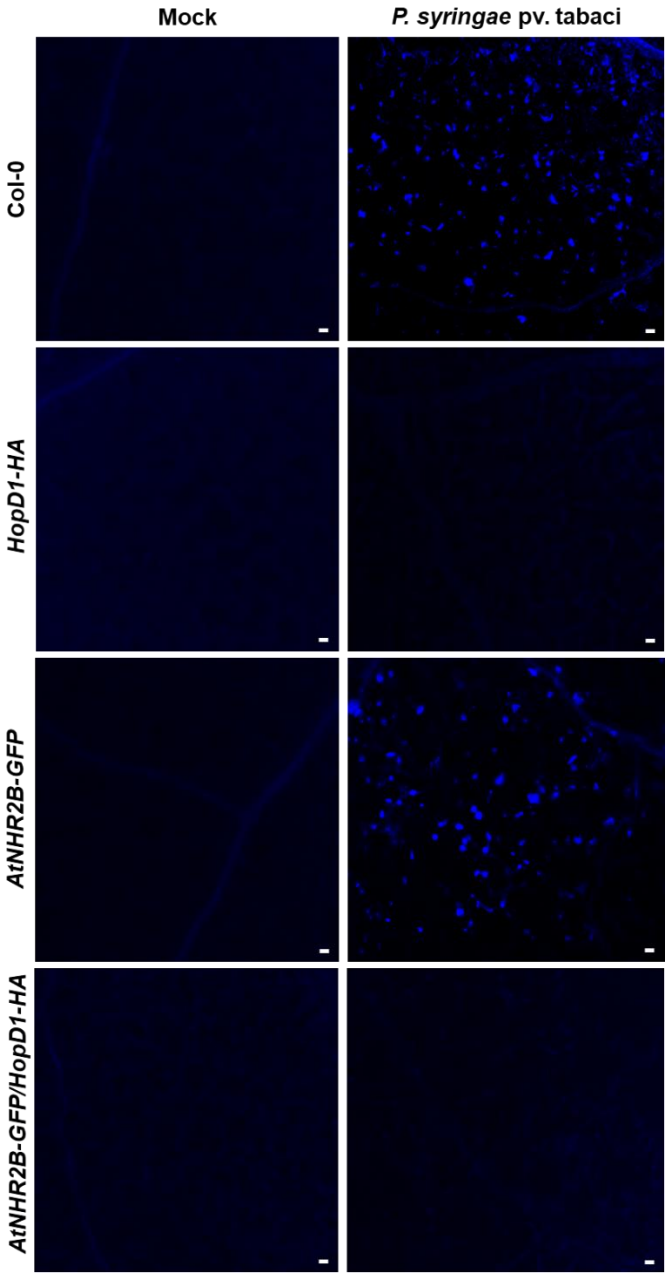

Figure 4. *Arabidopsis* plants expressing the bacterial effector *HopD1-HA* are deficient in callose deposition. Wild-type Col-0 and transgenic plants expressing *HopD1-HA, AtNHR2B-GFP* and *AtNHR2B-GFP/HopD1-HA* were syringe-inoculated with the non-adapted bacterial pathogen *P. syringae* pv. tabaci at OD_{600}= 0.02 (1 x 10^7CFU/mL) or mock-treated with water. Leaves were detached at 24 hpi and stained aniline blue. Images were taken using a confocal microscopy under DAPI filter. Scale bar= 20µm.

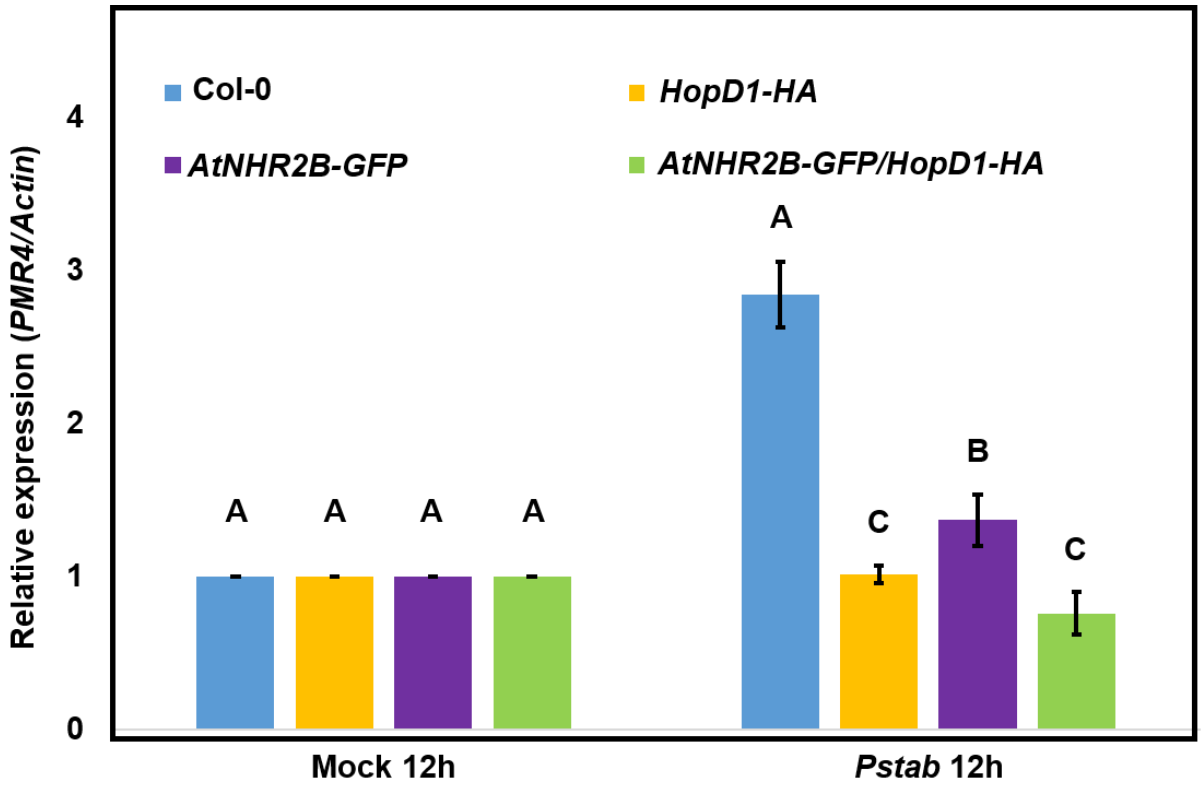

Figure 5. *PMR4* expression was reduced in *Arabidopsis* plants over-expressing the bacterial effector HopD1-HA. Tissue from Col-0, *HopD1-HA, AtNHR2B-GFP* and *AtNHR2B-GFP/HopD1-HA* plants inoculated with *P. syringae* pv. tabaci (10^7CFU/mL) was collected 24 hpi. *Arabidopsis* plants expressing *HopD1-HA* and *AtNHR2B-GFP/HopD1-HA* showed significant reduction of PMR4 expression. One-way ANOVA was used to test significant differences. Letter represent significant difference with $P \leq 0.05$. Same letters above bars indicate not statistically significant difference.

5 Conclusion

P. syringae pv. tomato DC3000 effectors HopD1 and HopG1 target the nonhost associated protein AtNHR2B. Both effectors caused different phenotypes upon inoculation with the non-adapted pathogen *Pstab*. *HopD1-HA* expressed alone or in combination with *AtNHR2B-GFP* caused developed of disease symptoms and higher bacterial proliferation. Furthermore, the expression of *HopD1-HA* inhibited the plant from depositing callose and downregulated the expression of the callose synthase gene *PMR4*. Further experiments are needed in order to understand the ways in which HopD1 targets the callose deposition pathway and interferes with the plant immune response.

In contrast, *HopG1-FLAG* expression was associated with the development of a HR accompanied by high levels of electrolyte leakage and elevated mitochondrial ROS production. Moreover co-expression of *HopG1-FLAG* and *AtNHR2B-GFP* caused development of disease symptoms and enhanced bacterial growth. ROS levels as well as electrolyte leakage levels were low compared to *HopG1-FLAG* expressing plants. Together these results indicate that: HopG1 acts as an avirulence determinant in absence of the target AtNHR2B, and that the presence of AtNHR2B is needed for the effector to promote bacterial virulence. Further experiments are needed to clarify if HopG1 acts in fact as an avirulence determinant.